

ULTRA SLOW OSCILLATIONS IN  
CORTICAL CULTURES

MOK SIEW YING

DOCTOR OF PHILOSOPHY IN ENGINEERING

FACULTY OF ENGINEERING AND SCIENCE  
UNIVERSITI TUNKU ABDUL RAHMAN  
DECEMBER 2012



**ULTRA SLOW OSCILLATIONS IN  
CORTICAL CULTURES**

By

**MOK SIEW YING**

1.

A thesis submitted to the Department of Mechatronics and  
Biomedical Engineering,  
Faculty of Engineering and Science,  
Universiti Tunku Abdul Rahman,  
in partial fulfillment of the requirements for the degree of  
Doctor of Philosophy in Engineering  
December 2012

## ABSTRACT

Dissociated primary neuronal cultures growing on planar multi-electrode arrays (MEAs) are promising tools used in the studies of network physiology. In my present work, small cultured neuronal networks from cortices of embryonic rats were grown and studied. The cortical cells formed extensive synaptic connections and became spontaneously active within days after plating, of which their bioelectrical activity could be tracked and recorded non-invasively.

Conventional drop-seeding technique has been widely used for preparing high-density cultures on MEAs. This is readily accomplished with freshly dissociated cells by spinning and proportional dilution of a concentrated cell suspension to the desired plating density. However, if cryopreserved neurons are used, the undesirably low viability of these neurons often leads to unsatisfactory plating density. To address this deficiency, a new seeding device for increasing and controlling the plating density of the neural cell suspension was developed. This device had greatly facilitated the preparation of successful primary cultures from cryopreserved neurons, with a large number of cells confined to the electrode regions of the MEAs for optimal recordings.

The electrodes on the MEAs are bi-directional and they can be used for both recording and stimulating action potentials. To enable stimulation of the cultured networks, a stimulator that interfaces with our existing recording

system was developed. The stimulator is capable of producing stimuli to reliably evoke action potential responses from neuronal ensembles in the arrays with minimal interference to the extracellular recordings.

Cortical cultures exhibit a surprisingly wide range of bursting activities that are relatively unstructured during most of their lifetime. Most remarkably, in my experiments, a new form of bursting activity was observed. The cortical networks of the monitored cultures regularly show a synchronous increase in their firing rates lasting a few minutes, constituting a very slow oscillatory activity ( $<0.01$  Hz). This form of oscillatory activity was seen in cortical cultures starting from the fourth week *in vitro*. Clustering analysis revealed conserved patterns of burst propagation that were recurrently occurring across successive oscillation cycles. By comparing the differences in the motif repetition between multi-unit and single-unit activities, the consistency of the burst motifs was found to be more robust at the electrode level compared to the neuronal level.

The work was concluded by studying the susceptibility of the ultra-slow oscillatory activity to electrical stimulation. The cultures were probed with low-frequency electrical stimuli and the changes induced in the distribution of different burst motifs were investigated. The activity recorded after stimulation resulted in greater changes in the occurrences of bursts belonging to different clusters than the spontaneously occurring changes, indicating a collective regulation in the network activity by electrical stimulation.

## ACKNOWLEDGEMENTS

There are many people to whom I am grateful for helping me throughout these years of my research. I would like to start by thanking my supervisor, Prof. Goh Sing Yau. Being a great mentor, he has given me tremendous freedom to choose my direction of research, yet always been available for advice and help. Without his enthusiasm in brain science research, I would have never made it through this project. I am also grateful to my co-supervisor, Dr Lim Yang Mooi for her patience and guidance, especially at the initial stage when I just started to learn about culturing cells.

I am truly blessed having a chance to work under Prof Jerry Pine for an academic placement at Caltech. Though the time was short, I have greatly benefited from his vast knowledge and wisdom. It was through his kindness that I was able to try out many state-of-the-art technologies that I have never experienced before. Thanks also to Ms Sheri McKinney for her guidance on cell preparation, and her continued help and advice after I have left Caltech.

Next, I'd like to thank Dr Lo Fook Loong and Dr Tan Eng Kiang for their valuable inputs to this project. I am also thankful to my fellow friends at UTAR, especially my group members – Danny, Siow Cheng, Lee Fan, Justin, Vincent, Raja Kumar and Yin Qing for their help and friendship.

Last, but certainly not least, I would like to express a special appreciation to my family for their unwavering support and encouragements. And also to my husband, for his immense patience and understanding.

*Financial support for this work was provided by the Chang Ming Thien Foundation and Fundamental Research Grant Scheme.*

## APPROVAL SHEET

This thesis entitled “**ULTRA SLOW OSCILLATIONS IN CORTICAL CULTURES**” was prepared by MOK SIEW YING and submitted as partial fulfillment of the requirements for the degree of Doctor of Philosophy in Engineering at Universiti Tunku Abdul Rahman.

Approved by:

---

(Prof. Dato’ Dr. Goh Sing Yau)  
Date:.....  
Professor/Supervisor  
Department of Mechanical and Material Engineering  
Faculty of Engineering and Science  
Universiti Tunku Abdul Rahman

---

(Assoc. Prof. Dr. Lim Yang Mooi)  
Date:.....  
Associate Professor/Co-supervisor  
Department of Pre-clinical Sciences  
Faculty of Medicine and Health Sciences  
Universiti Tunku Abdul Rahman

**FACULTY OF ENGINEERING AND SCIENCE  
UNIVERSITI TUNKU ABDUL RAHMAN**

Date: \_\_\_\_\_

**SUBMISSION OF THESIS**

It is hereby certified that **MOK SIEW YING** (ID No: **07UED08782**) has completed this thesis entitled “ULTRA SLOW OSCILLATIONS IN CORTICAL CULTURES” under the supervision of Prof. Dato’ Dr. Goh Sing Yau (Supervisor) from the Department of Mechanical and Material Engineering, Faculty of Engineering and Science, and Assoc. Prof. Dr. Lim Yang Mooi (Co-supervisor) from the Department of Pre-clinical Sciences, Faculty of Medicine and Health Sciences.

I understand that University will upload softcopy of my thesis in pdf format into UTAR Institutional Repository, which may be made accessible to UTAR community and public.

Yours truly,

\_\_\_\_\_  
(MOK SIEW YING)

## DECLARATION

I hereby declare that the thesis is based on my original work except for quotations and citations which have been duly acknowledged. I also declare that it has not been previously or concurrently submitted for any other degree at UTAR or other institutions.

Name MOK SIEW YING

Date \_\_\_\_\_

## TABLE OF CONTENTS

	<b>Page</b>
<b>ABSTRACT</b>	<b>ii</b>
<b>ACKNOWLEDGEMENTS</b>	<b>iv</b>
<b>APPROVAL SHEET</b>	<b>vi</b>
<b>SUBMISSION OF THESIS</b>	<b>vii</b>
<b>DECLARATION</b>	<b>viii</b>
<b>TABLE OF CONTENTS</b>	<b>ix</b>
<b>LIST OF TABLE</b>	<b>xii</b>
<b>LIST OF FIGURES</b>	<b>xiii</b>
<b>LIST OF ABBREVIATIONS</b>	<b>xv</b>
<b>CHAPTER</b>	
<b>1.0 INTRODUCTION</b>	<b>1</b>
<b>2.0 SEEDING DEVICE</b>	<b>6</b>
2.1 Introduction	7
2.2 A Device for High-density Seeding	8
2.3 Materials and Methods	10
2.3.1 Culture Preparation	10
2.3.2 Recording Electrical Signals	12
2.3.3 Spike Detection	13
2.3.4 Burst Detection	14
2.3.5 Synchrony	14
2.4 Results	15
2.4.1 Regulation of Seeding Density	15
2.4.2 Development of Spontaneous Activity	18
2.5 Discussion	27
2.6 Conclusion	29
<b>3.0 A MULTI-SITE ELECTRICAL STIMULATOR FOR SUBSTRATE INTEGRATED MULTI-ELECTRODE ARRAYS</b>	<b>30</b>
3.1 Introduction	30
3.2 A Multi-site Electrical Stimulator	32
3.3 Methods	36
3.3.1 Cell Culture	36
3.3.2 Recording	36
3.3.3 Electrical Stimulation	37

3.4	Results	37
3.4.1	Measured Specifications	37
3.4.2	Evoking Neuronal Responses with Extracellular Stimuli	39
3.5	Discussion	42
<b>4.0</b>	<b>ULTRA-SLOW OSCILLATIONS</b>	<b>44</b>
4.1	Introduction	44
4.2	Experimental Procedures	46
4.2.1	Cell Culture	46
4.2.2	Electrical Recording and Stimulation	47
4.2.3	Spike Detection and Sorting	48
4.2.4	Burst Detection	49
4.2.5	Periodicity	49
4.2.6	Similarity Indices	49
4.3	Results	50
4.4	Discussion	64
<b>5.0</b>	<b>RECONFIGURATION OF THE BURST COMPOSITION OF ULTRA-SLOW OSCILLATORY ACTIVITY BY LOW-FREQUENCY STIMULATION</b>	<b>67</b>
5.1	Introduction	68
5.2	Methods	69
5.2.1	Cell Culture	69
5.2.2	Recording	70
5.2.3	Electrical Stimulation	70
5.2.4	Burst Detection	71
5.2.5	Detection of Burst Motifs	71
5.2.6	Quantifying Changes in Burst Composition	73
5.3	Results	74
5.3.1	Identifying Recurring Burst Motifs across Stimulation	79
5.3.2	Reconfiguration of the Burst Composition of Ultra-slow Oscillatory Activity	81
5.4	Discussion	84
<b>6.0</b>	<b>CONCLUDING REMARKS AND FUTURE DIRECTION</b>	<b>87</b>
6.1	Summary of Major Results	87
6.1.1	Seeding Device	87
6.1.2	Ultra-slow Oscillations	88
6.2	Future Direction: Towards a Better Understanding of the Ultra-slow Oscillations	90
6.2.1	Pharmacology	90
6.2.2	Lithography	91

<b>REFERENCES</b>	<b>92</b>
<b>APPENDIX A</b> Culturing Methods	<b>100</b>

## LIST OF TABLE

<b>Table</b>		<b>Page</b>
2.1	Plating parameters	11

## LIST OF FIGURES

Figures		Page
2.1	Diagram showing the device coupled to an MEA chamber for seeding cells at high density	9
2.2	Phase contrast micrographs of dissociated cortical neurons cultivated on MEAs	17
2.3	Developmental changes in spontaneous network activity	20
2.4	Fraction of active electrode computed at various ages <i>in vitro</i>	22
2.5	Development of activity in cultures	23
2.6	Histograms designating the distribution probability of burst sources	25
2.7	Gray scale representation of the cross-correlation coefficients ( $r$ ) computed between a reference electrode and each of other electrodes in three independent cultured networks on different days <i>in vitro</i>	26
3.1	The multi-site electrical stimulator	34
3.2	Screenshot from the oscilloscope showing a blanking (TTL) pulse and a biphasic voltage pulse	35
3.3	Evoked response recorded at a non-stimulated site	39
3.4	Raster plot showing the array-wide responses following stimulation on a single electrode for 20 trials	41
4.1	Ultra-slow oscillations in cortical cultures	52
4.2	Identifying burst motifs in the multi-unit activity	54
4.3	Distinct spatiotemporal patterns of burst propagation	58
4.4	Identifying burst motifs in the single-unit activity	60
4.5	Burst propagation latency as a function of burst size	63

5.1	Ultra-slow oscillations	75
5.2	Identifying repeating burst motifs in the ultra-slow oscillatory activity in three randomly selected cultures	76
5.3	Distinct propagation patterns of bursts at peaks and troughs	80
5.4	Distribution of bursts from different motifs across stimulation	82
5.5	Comparison of spontaneous changes and changes concomitant with stimulation in the burst composition	84
A.1	Photograph showing the amplifier placed on top of the custom-made heat exchanger	103

## LIST OF ABBREVIATIONS

ASDR	array-wide spike detection rate
DIV	days <i>in vitro</i>
FFT	fast Fourier transform
IBI	inter-burst interval
ISI	inter-spike interval
MEA	multi-electrode array
PCA	principal component analysis
PEI	poly-ethylene-imine
RMS	root-mean-square

## CHAPTER 1

### INTRODUCTION

The brains are the center of our biological and cognition functions. Thus, neurons, and the neuronal networks they form, have been the subjects of intense interest to many scientists. However, these entities are difficult to approach due to the location in which they reside and the complexity of the system on the whole. As a result, considerable efforts have been devoted to the study of simpler, reduced systems. One of these systems is that of vertebrate neuronal cell culture, which has been extensively utilized in many neurobiological studies, as well as the work described in this thesis.

Dissociated vertebrate neurons can be grown in cultures for many months (Banker and Goslin 1998; Potter and DeMarse 2001). When plated onto substrates, neurons readily grow out via axo-dendritic processes and proceed in cultures to form elaborate networks. Electrical activity starts to develop after a few days *in vitro*. These activities, including sporadic spikes and network bursts continue to develop throughout the lifetime of the cultures. With proper care and maintenance, therefore, these cultures serve as an excellent model in which the dynamics of neuronal growth and firing activity can be followed. Many studies have been made in this direction, which have yielded very valuable data of their characteristic changes at different developmental stages (Ramakers et al., 1991; van Ooyen et al., 1995; Voigt et

al., 1997; Corner et al., 2002; van Pelt et al., 2005; Wagenaar et al., 2006b), as well as on how the network dynamics vary when manipulated with electrical stimuli or pharmacological agents (Canepari et al., 1997; Maeda et al., 1998; Latham et al., 2000).

Studying neuronal networks in cultures offers many advantages over *in vivo* approaches. Apart from their mechanical stability, cultured networks are much more accessible to microscopic imaging compared to their *in vivo* counterparts. Additionally, they also provide better pharmacological specificity and experimenter's control over the extracellular environment. Although these networks do not possess the 3-dimensional architecture of real brains, their structure of connectivity is not random. In fact, there is evidence that cultured networks sometimes exhibit small-world like architecture (Shefi et al., 2002). This view is further strengthened with the demonstration of repeating motifs in the neuronal firing activities in the dissociated cultures (Segev et al., 2004; Wagenaar et al., 2006a; Rolston et al., 2007). All the above studies, either direct examination of the network organization of small neuronal cultures, or investigation of their firing dynamics, are extremely useful to advance our understandings of the development and organization processes of *in vivo* networks.

Our present work focuses on the oscillatory dynamics in dissociated cultures, a study that many researchers consider to be important for providing more insights into neuronal networks. Indeed, previous investigations on the rhythmic firing dynamics of cultures under both spontaneous and stimulated

conditions (Maeda et al., 1995; Gross et al., 2000; Opitz et al., 2002; Zhu et al., 2010) have led to many critical details underlying neuronal oscillations that are otherwise difficult to access *in vivo*. Much knowledge has also been gained from endeavors to induce oscillations in cultures through different means, among which includes blocking of inhibition (Misgeld et al. 1998; Gross et al., 2000; Streit et al., 2001), enhancement of synaptic transmission (Murphy et al., 1992; Robinson et al., 1993; Streit et al., 2001), and prolonged inhibition of glutamatergic neurotransmission (Furshpan and Potter 1989). We hope that the present investigations of the dynamics of the ultra-slow oscillations in cortical networks can help to further elucidate the mechanisms of neuronal oscillations.

In this thesis, we presented the studies of oscillatory dynamics of cortical cultures growing on multi-electrode arrays (MEAs) – two-dimensional arrays of electrodes on glass or silicone substrates. One obvious prerequisite for using this technique to study cultured networks is, of course, that the neurons must be located in close proximity to the electrodes. Adapting the conventional drop-seeding technique for seeding cells on the arrays is not practical when the concentration of the cell suspension is too low. This eventually led to the development of a new seeding device to facilitate preparation of high-density cultures on MEAs. In the second half of this thesis, the oscillatory dynamics of cortical cultures were investigated, with emphasis given to the internal structure of the network bursts. Analysis of the data obtained from these studies was built on a standard clustering algorithm to search for repeating motifs across the oscillatory activity. Additionally,

changes in the spatiotemporal dynamics across the ultra-slow oscillations after electrical stimulation were studied.

The rest of this thesis is organized as follows:

Chapter 2 provides a description of the device used to facilitate high-density seeding of dissociated neuronal cells on MEAs. To better appreciate its effectiveness, comparison is made between the aggregate firing rates recorded from cultures grown with and without the aid of the device. More network characteristics of the high-density cultures prepared with the device are shown and discussed in the latter part of this chapter.

Chapter 3 presents the design of our multi-site electrical stimulator. The chapter provides the results of several important performance measures of the stimulator, and shows evidence that stimulation sequences delivered extracellularly through the substrate electrodes are effective and reliable.

Chapter 4 describes an ultra-slow oscillation that spontaneously emerged in cortical cultures during the late developmental phase. Findings of its underlying dynamics are presented, with emphasis given to the internal structure of firing patterns within the network bursts. The consistency of its multi-unit activity and single-unit activity is also discussed.

Chapter 5 discusses the effect of electrical stimulation on the ultra-slow oscillations described in Chapter 4. Changes in the composition of bursts with

varying spatiotemporal substructures of networks under stimulation are quantified and compared with the spontaneous changes in the networks.

Chapter 6 concludes this thesis with a summary of findings from the previous chapters. Some suggestions for future work are also proposed and discussed here.

## CHAPTER 2

### SEEDING DEVICE\*

A device to facilitate high-density seeding of dissociated neural cells on planar MEAs is presented in this chapter. The device comprises a metal cover with two concentric cylinders – the outer cylinder fits tightly on to the external diameter of an MEA to hold it in place and an inner cylinder holds a central glass tube for introducing a cell suspension over the electrode area of the MEA. An O-ring is placed at the bottom of the inner cylinder and the glass tube to provide a fluid-tight seal between the glass tube and the MEA electrode surface. The volume of cell suspension in the glass tube is varied according to the desired plating density. After plating, the device can be lifted from the MEA without leaving any residue on the contact surface. The device has enabled us to increase and control the plating density when using neural cell suspensions with low viability, and to prepare successful primary cultures from cryopreserved neurons and glia. The cultures of cryopreserved dissociated cortical neurons that we have grown in this manner remained spontaneously active over months, and exhibited stable development and similar network characteristics as reported by other researchers.

---

\* Published as: S. Y. Mok, Y. M. Lim, and S. Y. Goh, 2009: A device to facilitate preparation of high-density neural cell cultures in MEAs. *J. Neurosci. Methods*. **179**, pp. 284-291.

## 2.1 Introduction

Dissociated primary neuronal cultures growing on planar MEAs are promising tools used in the studies of network physiology (Maeda et al., 1995; Kamioka et al., 1996; Potter and DeMarse 2001; Marom and Shahaf 2002; Eytan et al., 2003; Jimbo et al., 2006; Wagenaar 2006; Pasquale et al., 2008). This experimental system provides a powerful platform for *in vitro* electrophysiology, allowing multi-site, long-term and non-invasive extracellular recordings from neurons cultured on different regions of the arrays.

In recent years, primary cryopreserved embryonic neurons have become commercially available, and have been used for investigations of network activity on MEAs (Otto et al., 2003; Linke et al., 2006). Cryopreserved neurons are indistinguishable from freshly dissociated neural cells, with both exhibiting similar morphological and electrophysiological properties (Otto et al., 2003). These ready-to-use cryopreserved resources omit the need for serial preparation and cultivation of primary cells, rendering great simplicity to the culturing process. However, it is difficult to maintain high cell viability in these cryopreserved neurons, which, in turn, leads to unsatisfactory plating density.

We developed a device to address this deficiency, by confining the neurons to grow at the electrode regions of the MEAs. Unlike the commercially available cloning cylinders employed by other researchers

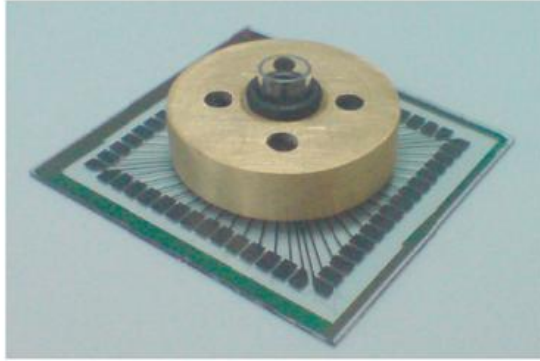
(Streit et al., 2001), the use of silicone sealant at the electrode surface is precluded in our design, in order to prevent damages to the electrode tracks when the cylinders are removed. To further verify the efficiency of this method, spontaneous developmental changes of the cortical networks cultivated on planar MEAs were monitored and studied.

## **2.2 A Device for High-density Seeding**

One prerequisite for recording extracellular signals from planar MEAs is that the neurons must be located in close proximity to the electrodes (Claverol-Tinture and Pine 2002). This can be achieved with cells plated at high density (2000 cells/mm<sup>2</sup>), which is also required to ensure a healthy culture development and neuronal survival after cryopreservation (Kawamoto and Barrett 1986; Marom and Shahaf 2002). However, due to prolonged shipping (5-6 days) and difficulties dealing with cold chain maintenance during delivery, our cryopreserved neurons usually showed an undesirably low percentage of viability. An assessment of cell viability carried out using trypan blue method revealed only ~15% of viable cells.

Since our preparation demanded a higher concentration of viable cells (~10<sup>6</sup> cells/ml) than the initial suspension, it led us to develop a device for restricting cells to the central electrode region of the MEAs, as described below.

A



B

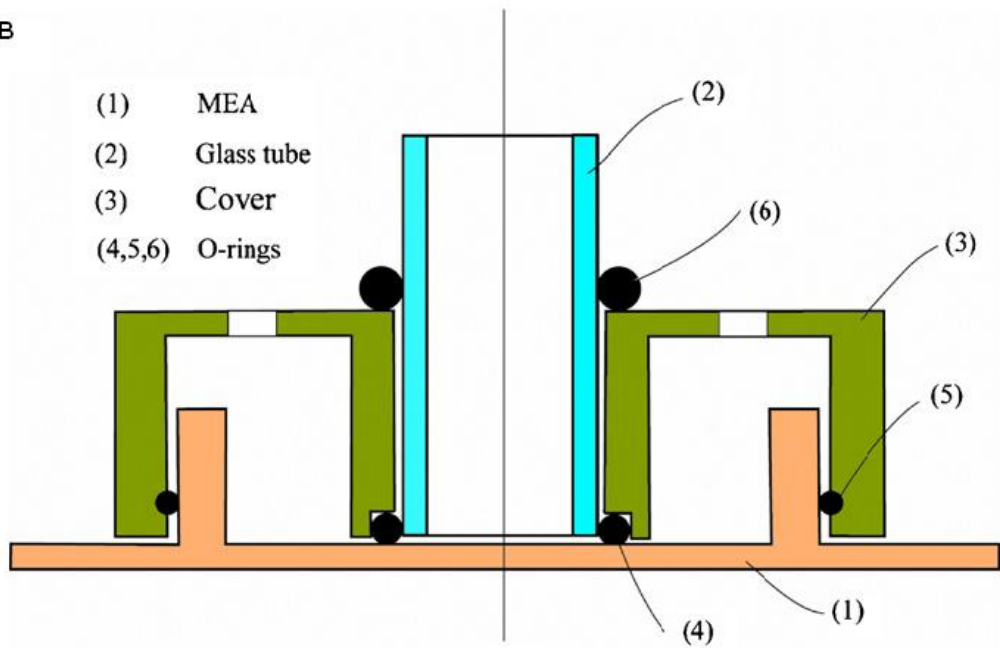


**Figure 2.1:** Diagram showing the device coupled to an MEA chamber for seeding cells at high density. O-ring in the inner groove forms a liquid tight seal between the glass tube and the electrode surface. A. Photograph. B. Cross-sectional diagram.

Figure 2.1 shows a device developed to increase plating density of viable cells at the electrode area of the MEAs. The device consists of a cover accommodating a thin glass tube (13 mm height, 5.5 mm inner diameter) at the center. The glass tube covers the central electrode area of the MEA that we wish to deposit the neurons. The cover consists of 2 concentric rings. The inner surface of the outer ring fits tightly to the MEA with the use of a rubber O-ring (5) placed in a groove. A second O-ring (4) at the bottom of the inner ring of the cover provides a liquid tight seal between the glass tube and the electrode surface. As the cover is pressed down to fit the MEA, the O-ring is at the same time pressed to form a good seal with the electrode surface. This seal prevents fluid inside the glass tube from leaking out of the MEA electrode area. In this manner, a larger volume containing a sufficient number of viable cells can be attained in the glass tube. The cells are allowed to settle onto the MEA electrode area before the cover is removed. Another thicker O-ring (6) is placed at the top of the assembly to hold the glass tube in place. This allows the whole assembly to be lifted up and away from the MEA, without leaving any residue on the substrate.

## **2.3 Materials and Methods**

### **2.3.1 Culture Preparation**

Dissociated cultures were prepared from Rat Brain Cortex Neuronal Cells (R-CX-500, Lonza, USA), which contained approximately 4 million viable cells

**Table 2.1:** Plating parameters.

	With device	Without device
Concentration of viable cells in suspension (cells/ $\mu$ l)	150	150
Plating volume ( $\mu$ l)	300	300
Number of cells/chamber	45,000	45,000
Plating diameter (mm)	5.5	19
Plating density (cells/mm <sup>2</sup> )	~2,000	~160

in a single vial prior to cryopreservation. Upon thawing, the cell suspension (1 ml) was slowly diluted with 3 ml Neurobasal medium (Invitrogen) supplemented with 10% Equine serum (HyClone), 2% B27 (Invitrogen) and 0.5 mM Glutamax (Invitrogen). It was then resuspended by gentle inversion for two times.

Prior to seeding, we pre-coated the MEAs with poly-ethylene-imine (PEI) (Lelong et al., 1992) and laminin, as previously reported (Potter and DeMarse 2001). We then fixed the device onto the MEA chambers immediately after the laminin drops were removed by vacuum suction. Subsequently, 300  $\mu$ l of the cell suspension was added drop-wise into the glass tube at the central electrode region of each MEA, and the dishes were immediately transferred to the incubator. In addition to that, control cultures were also prepared on the coated MEAs in the absence of the device. Table 2.1 summarizes the plating parameters used in our preparation.

The cells were allowed to settle on the substrates for 4 h before the device was lifted. All the cultures, including the controls were then rinsed gently in plating medium prior to the addition of 1 ml new medium. The dishes were

sealed with FEP Teflon<sup>®</sup> lids (Potter and DeMarse 2001) and kept in a dry incubator (60–70% RH, 5% CO<sub>2</sub>/95% air) at 37 °C. They were maintained in serum-free Neurobasal medium after 4 days *in vitro* (DIV), with half medium change performed twice a week. No antimitotic drug was added to restrict glia proliferation, as glial cells are known to be important for maintaining long-term culture health (Wagenaar 2006; Pasquale et al., 2008).

### **2.3.2 Recording Electrical Signals**

Neural cells were cultured on MEAs (MultiChannel Systems, Reutlingen, Germany) with 60 titanium nitride electrodes, 30 µm in diameter, laid out on an 8×8 grid with 200 µm inter-electrode spacing. The electrical signals detected were amplified using a commercial 60-channel amplifier (MEA1060-Inv-BC, MultiChannel Systems) with frequency limits of 10 Hz to 3 kHz and a gain of 1100×. Signals were sampled at 25 kHz using a data acquisition card (MC Card, MultiChannel Systems) at 14-bit resolution. Online visualization and spike detection were performed with MC Rack software (MultiChannel Systems), and spike trains were stored for offline processing using MATLAB.

To demonstrate the electrical functionality of the cultured networks, we monitored and recorded the spontaneous electrophysiological activity of the cultures starting from 6 DIV. Recordings were performed inside the same incubator used for maintaining cultures. The amplifier was placed on top of a custom-made heat exchanger that was water-cooled with running water from a

tap. In this manner excess heat was dissipated from the amplifier and the temperature of the MEA substrates was stabilized.

Before each recording session, the cultures were monitored for 15 min (Streit et al., 2001; Eytan et al., 2003) to ensure stability of the network activity. We also scheduled our recordings at least 12 h after feeding to avoid electrophysiological transients (Potter and DeMarse 2001; Wagenaar 2006).

### **2.3.3 Spike Detection**

Extracellular signals were often corrupted by noise from the recording hardware, interference from electromagnetic sources, as well as biological noise from superimposed activities of multiple and distant neurons (Mtetwa and Smith 2006).

To extract spikes from the background noise, the detected voltage traces were first high-pass filtered at 200 Hz to remove the low-frequency postsynaptic potential components, yielding a flat baseline for spike detection. Signals were then detected as online excursions beyond a threshold of  $\pm 5\sigma$ , with  $\sigma$  being the estimated root-mean-square (RMS) noise for each individual recording channel. As a spike was identified, subsequent spikes within the following 2 ms window were removed offline, in order to prevent duplicate detection of multiphasic spikes (Wagenaar 2006).

In this chapter, all analyses were performed based on multi-unit activity; no attempt was made to discriminate candidate spikes picked up by the same electrode (Eytan and Marom 2006; Wagenaar 2006).

#### **2.3.4 Burst Detection**

Bursts of activities were identified according to a method previously described (Wagenaar 2006). We first extracted sequences of at least four densely spaced spikes with a maximum inter-spike interval (ISI) of 100 ms as the core of a burst on individual electrodes. They were later extended to include entourage of spikes on the same electrodes with ISIs less than 200 ms. A network burst is then defined as an episode of temporally overlapping burst activities occurring across different channels over the entire network.

The arrival time of the initial spikes of each burst was stored, and the corresponding electrodes which were associated with the location of the burst initiation sites were identified (Cozzi et al., 2006; Eytan and Marom 2006).

#### **2.3.5 Synchrony**

To characterize the level of synchronization among electrodes in the networks, correlation analysis was performed between spike trains recorded by all electrode pairs (Tam 2000). We computed Pearson product correlation coefficients ( $r$ ) as described in the following formula:

$$r = \frac{\sum (x - \bar{x})(y - \bar{y})}{\sqrt{\sum (x - \bar{x})^2 (y - \bar{y})^2}},$$

where  $x$  and  $y$  represent the corresponding binned spike counts in the  $X$  and  $Y$  trains, respectively, using a bin size set at 10 ms. This equation yields the normalized covariance of spike firing rates, independent of the level of neuronal activity (Weliky and Katz 1999).

## **2.4 Results**

### **2.4.1 Regulation of Seeding Density**

Knowing the percentage of viability of cell suspension and the desired seeding density in the electrode area, we computed the required volume of suspension to be added in the glass tube of the device. The cells in the suspension settled on the electrode area at a speed that was determined by their weight. Individual viable cells with intact cytoplasm and heavier cell clumps settled faster and attached to the substrate. Dead cells and cell debris, which were relatively lighter, settled slower and formed clumps above the underlying layer of viable cells.

On removal of the plating medium, fractions of cell debris, dead cells and unattached intact cells were discarded, while some residues formed sticky aggregates and settled on the viable cells. It was difficult to achieve an entire living population inside the chambers; even by repeated rinsing, we failed to remove most of these unwanted constituents. However, the cell debris

eventually detached from the viable cells as the extracellular matrix on the cell membrane degraded, and was then removed during subsequent medium changes. Viable cells that were deposited onto the substratum formed a monolayer covering the electrode area, with cell bodies either attaching on to or close to the electrodes.

The cryopreserved embryonic neurons that were plated on the planar MEAs demonstrated the capacity to form intact networks. Starting from a population of dissociated cells that appeared round or oval, they began to extend neurites within several hours after plating, and continued to form numerous synaptic connections. Usually neurons were terminally differentiated upon seeding (Potter 2001), while glial cells continued to divide and proliferate when maintained in cultures.

To further demonstrate the significance of incorporating the device in preparing high-density cultures, we compared cortical cultures cultivated on MEAs with and without using the device at different stages of development. Figure 2.2 shows that although an equal volume of cell suspension was added in both cases, the use of the device during cell seeding effectively concentrated cells at the electrode area leading to a definite increase in cell density. By contrast, in the latter case, cell suspension added to the central area of the MEA spread across the whole chamber due to its hydrophilic surface. The cells were so thinly distributed that they formed a network with sparse connectivity, resulting in substantially fewer cells deposited around the electrodes.

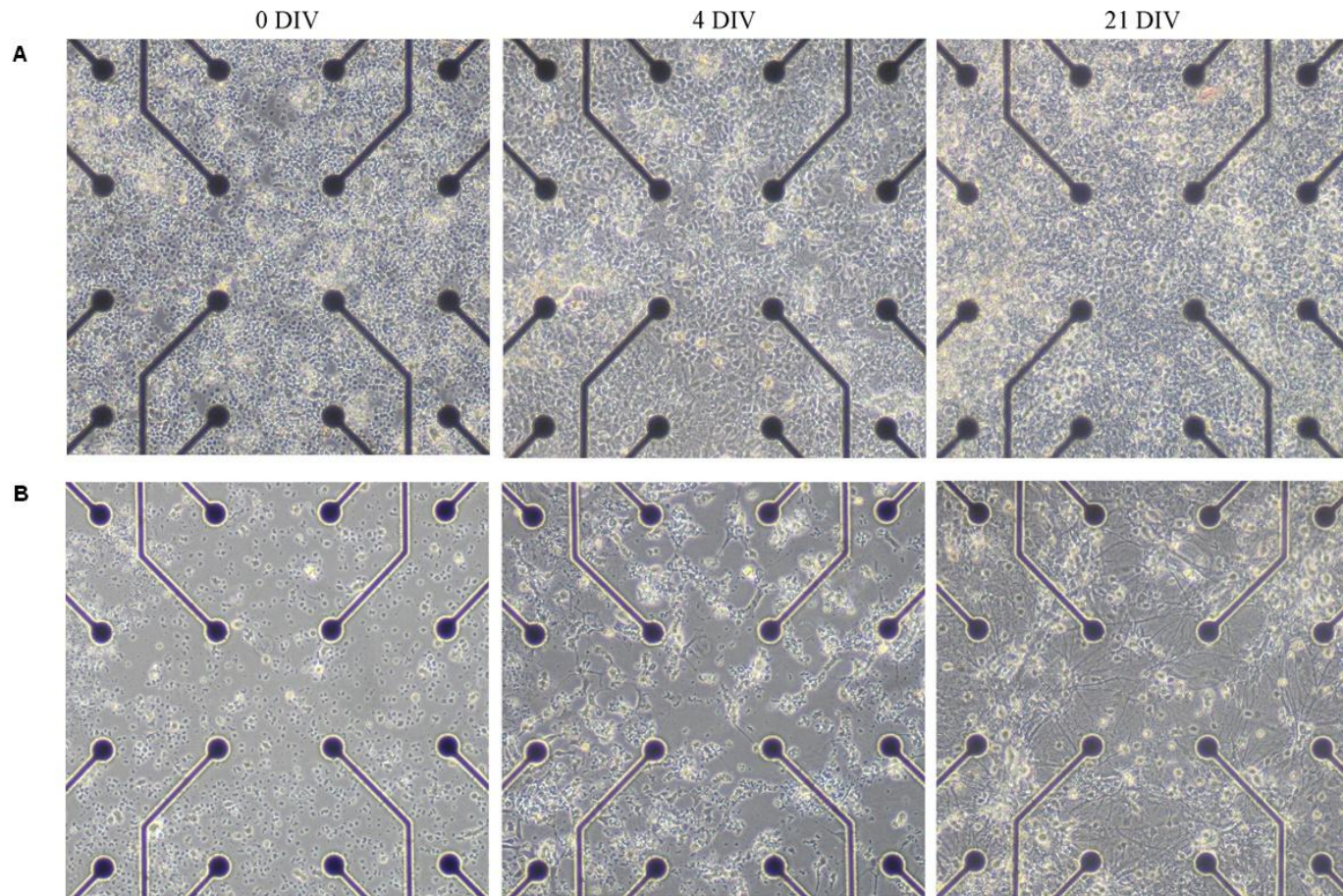


**Figure 2.2:** Phase contrast micrographs of dissociated cortical neurons cultivated on MEAs. A. With the aid of device. B. Without using the device. Scale: 200  $\mu\text{m}$  between electrodes.

Adding on to the distinct difference in network density, the survival rate of neurons was noticeably lower in the sparse control cultures (Segal et al., 1998). Successful recordings had been obtained in the high-density cultures for more than 1 month *in vitro* but were hardly possible to acquire in control cultures which mostly did not survive even during the premature stage. Optimization of the plating density made possible with the use of the device not only contributed to the survival of the cultures but also enhanced the detection of extracellular activity from the signal sources, as detailed in the following section.

#### **2.4.2 Development of Spontaneous Activity**

In the high-density cultures prepared with the aid of the device, electrical firings started to appear on a few electrodes during the first few days *in vitro*, in the form of uncorrelated random spiking. Local bursts involving a small number of electrodes were later detected, before they changed into the much more synchronized bursts. During the early immature stage, a slow propagation of burst activities which involved only a subset of electrodes at the neighboring sites was observed in most cultures. With maturation of the cultures, they evolved into array-wide synchronized bursts involving most of the active electrodes. Bursts at this stage travelled at higher velocity, denoting the increase in the number and maturation of the synapses (Maeda et al., 1995).

Synchronous regular bursting was mostly apparent during the second week *in vitro* (9–13 DIV), with bursts clustering into short groups separated by long

inter-burst intervals (IBIs) (Wagenaar 2006). In the later stage of development (more than 3 weeks after plating), the activity of the cultures evolved into complicated non-periodic, synchronous bursting which appeared to be largely unstructured. This activity persisted for another month, and thus represented the mature state of the networks (Kamioka et al., 1996; Marom and Shahaf 2002). The overview of the firing rate profile of a high-density culture prepared using the device is illustrated in Figure 2.3A.

On the contrary, spontaneous activity detected in the control cultures ( $N = 8$ , 3 plating batches) was much lower compared to the high-density cultures commensurate to fewer cells in the vicinity of the electrodes. The activity level was low throughout the development of the cultures, as illustrated in Figure 2.3B. It is worth noting that the control cultures exhibited different electrophysiological properties from high-density cultures, owing primarily to the reduced number of active neurons in the networks. Instead of intense bursting, extracellular recordings revealed mostly sporadic firings at the sites in contact with neural cells. In some of the control cultures, synchronized bursts were observed on the active electrodes. However, they usually began at a later time and were less frequent compared to bursting activity in the high-density cultures.

High-density seeding compensates for the deficiencies of neural cell cultures with low concentration, by improving both their electrophysiological activity and neuronal survival. This makes them particularly promising

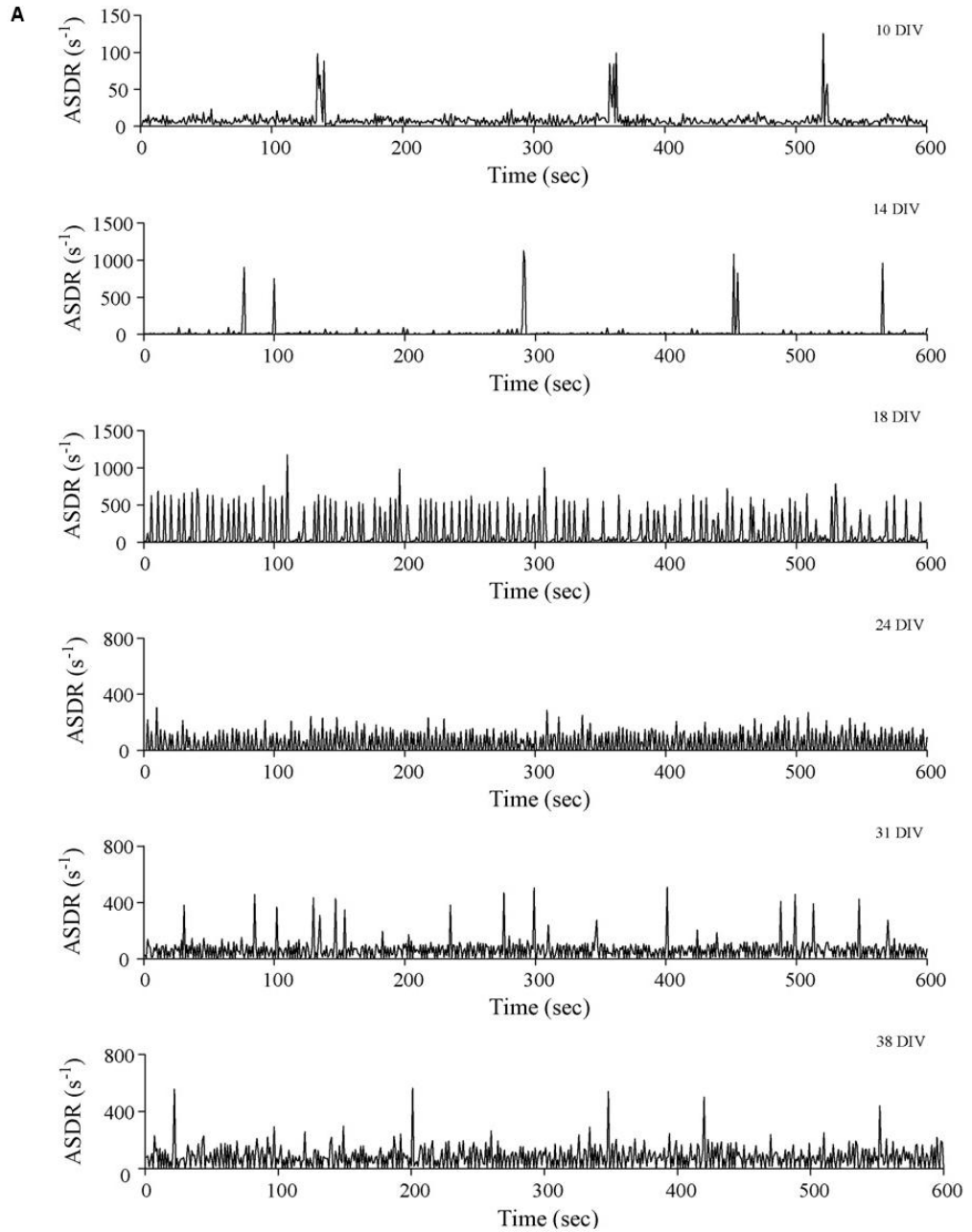


**Figure 2.3:** Developmental changes in spontaneous network activity. Graphs showing array-wide spike detection rate (ASDR) computed using one-second time bins from randomly selected cultures prepared (A) with the aid of device (B) without using the device.

(continued on next page)

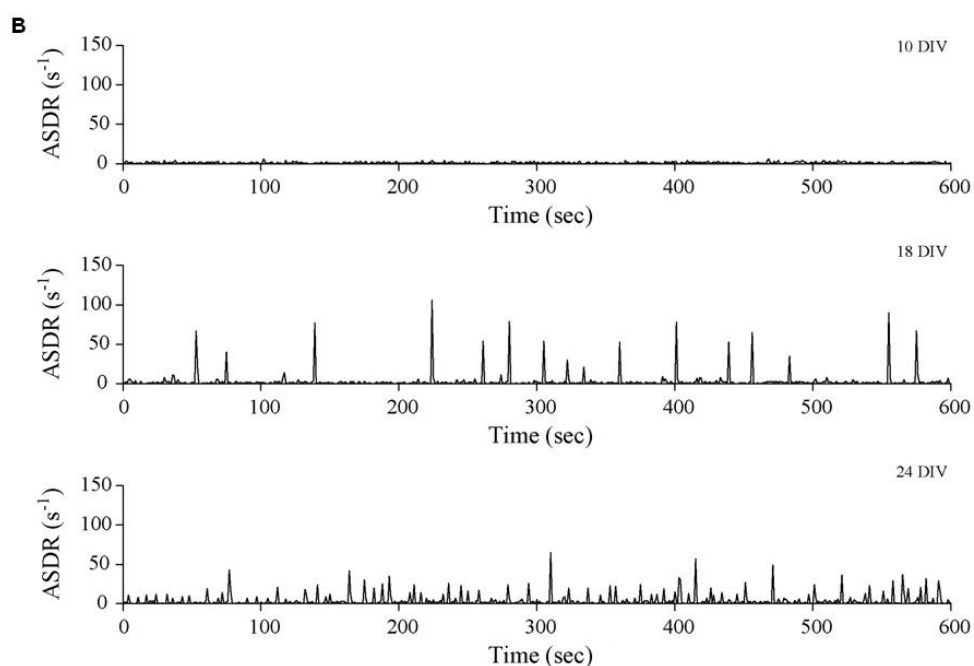


(Figure 2.3, continued)

in various studies which require stable monitoring over extended periods of time. For this reason, the rest of this section only focuses on further analyses to validate the properties of high-density cultures prepared using the device ( $N = 10$ , 3 plating batches).

Figure 2.4 depicts the changes in the number of active sites with culture age. We define an active electrode as the one demonstrating average firing rate above 0.02 Hz (Eytan and Marom 2006). It was evident that more electrodes became electrically active with culture age (Jimbo et al., 2006). Eventually most of the electrodes (80–90%) were recruited once bursts had started (from the second week onwards), and persisted throughout the development of the cultures.

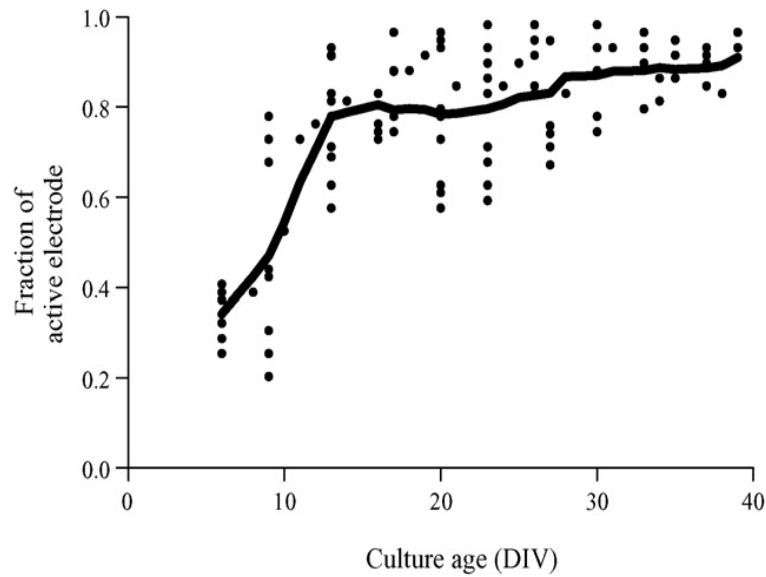


**Figure 2.4:** Fraction of active electrode computed at various ages *in vitro*. Each dot represents a measurement from individual cultures, and the line is the interpolated average.

Consistent with the findings of other researchers (Jimbo et al., 2006; Wagenaar 2006), the changes in the firing properties of the cultures were irregular throughout their development. Individual cultures exhibited different levels of spiking activities with varied development speeds, with cultures from different batches exhibiting diverse difference despite their same plating density. On average the mean firing rate across all cultures showed an increase with culture age (Figure 2.5A).

In most cultures, the mean burst frequency increased considerably starting from the second week *in vitro*, from approximately 0.02 to 0.6 Hz. The mean burst level of the cultures kept increasing as their activities were progressively dominated by network bursts. An extensive variety of burst patterns were observed in different cultures; the properties of the burst activities continued to change during the observation period.

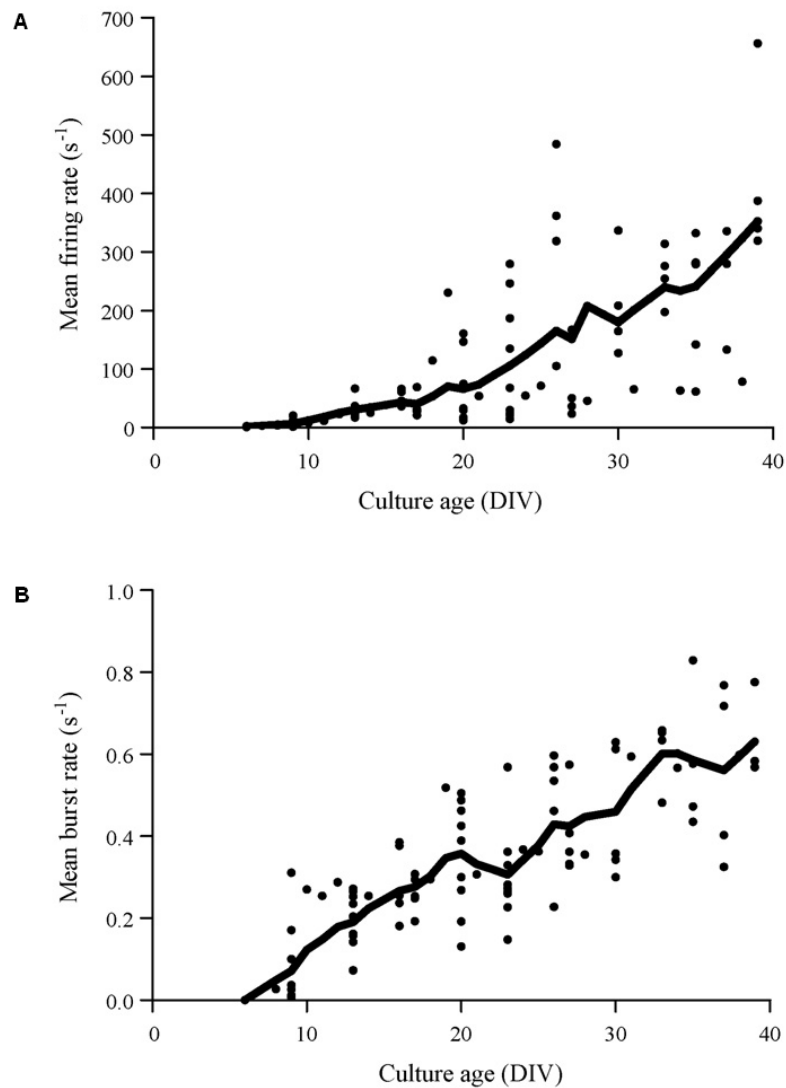


**Figure 2.5:** Development of activity in cultures. A. Mean firing rate. B. Mean burst rate. Each dot represents a measurement from individual cultures, and the line is the interpolated average.

We quantitatively analyzed the initiation sites during spontaneous network bursts, and observed that a subset of electrodes was reliably activated prior to other participating electrodes. Bursts in the early phase were observed at only a few distinctive sites. As the cultures matured, more of these distinctive burst initiation sites started to emerge. This implied an increase in the sensitivity of the neurons to the network activity with culture age, which was attributed to enhanced connectivity in the networks (Eytan and Marom 2006; Feinerman et

al., 2007). Bursts triggered at these initiation sources propagated via multiple synaptic pathways to affect larger neural cell populations in the networks (Feinerman et al., 2007). Figure 2.6 shows the distribution of spontaneous burst initiation sites from one of the randomly selected cultures on different days *in vitro*.

Synchronization among activity recorded at different electrodes in the networks was computed using the cross-correlation method. We randomly selected an active electrode in each culture to be the reference electrode, and calculated the correlation coefficients between the former with all other electrodes in the same network. As shown in Figure 2.7, correlation in the activity between electrode pairs in the networks increased with culture age, indicating the very simple fact of the increase in the synaptic density (Kamioka et al., 1996; Jimbo et al., 2006).

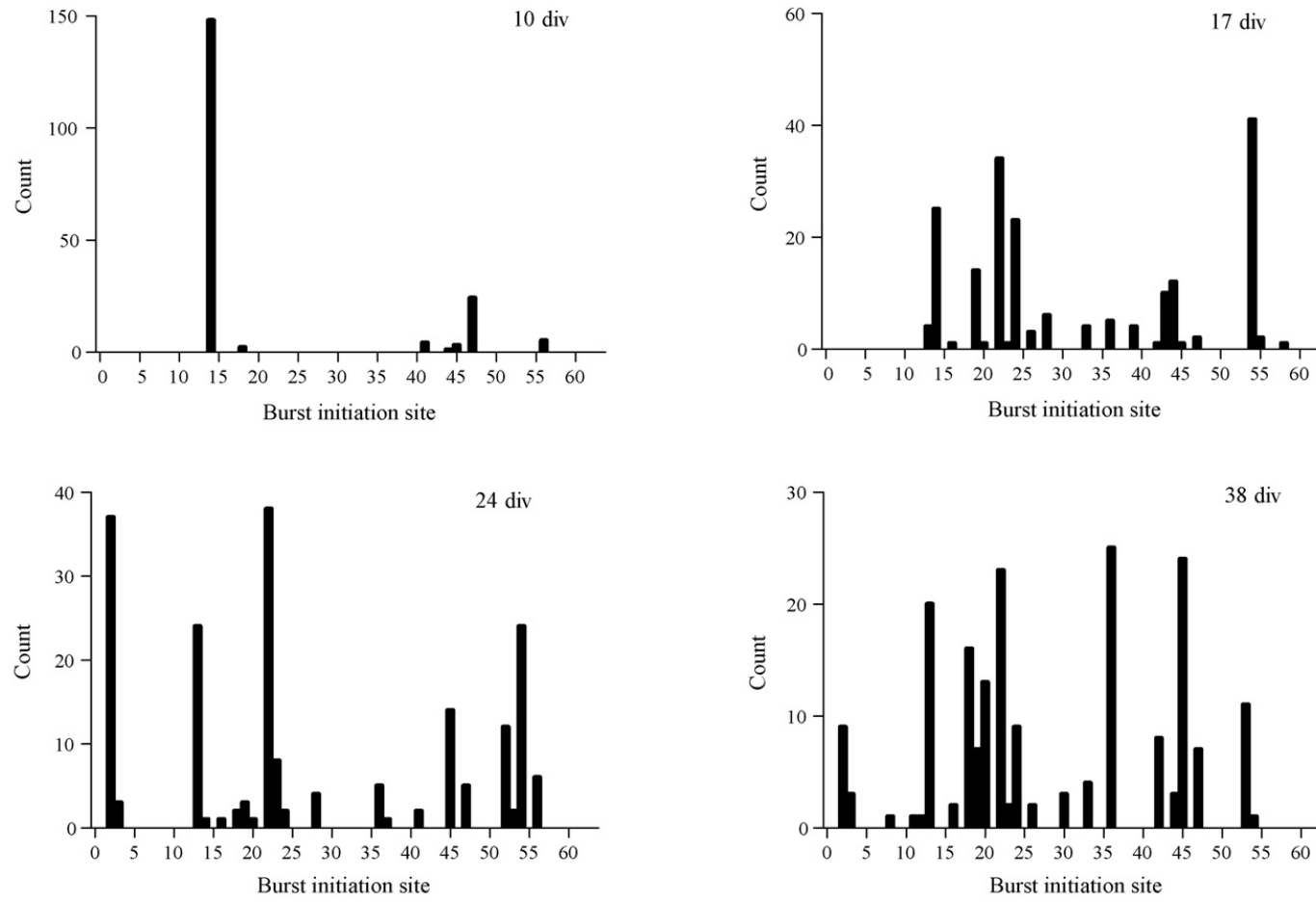


**Figure 2.6:** Histograms designating the distribution probability of burst sources.

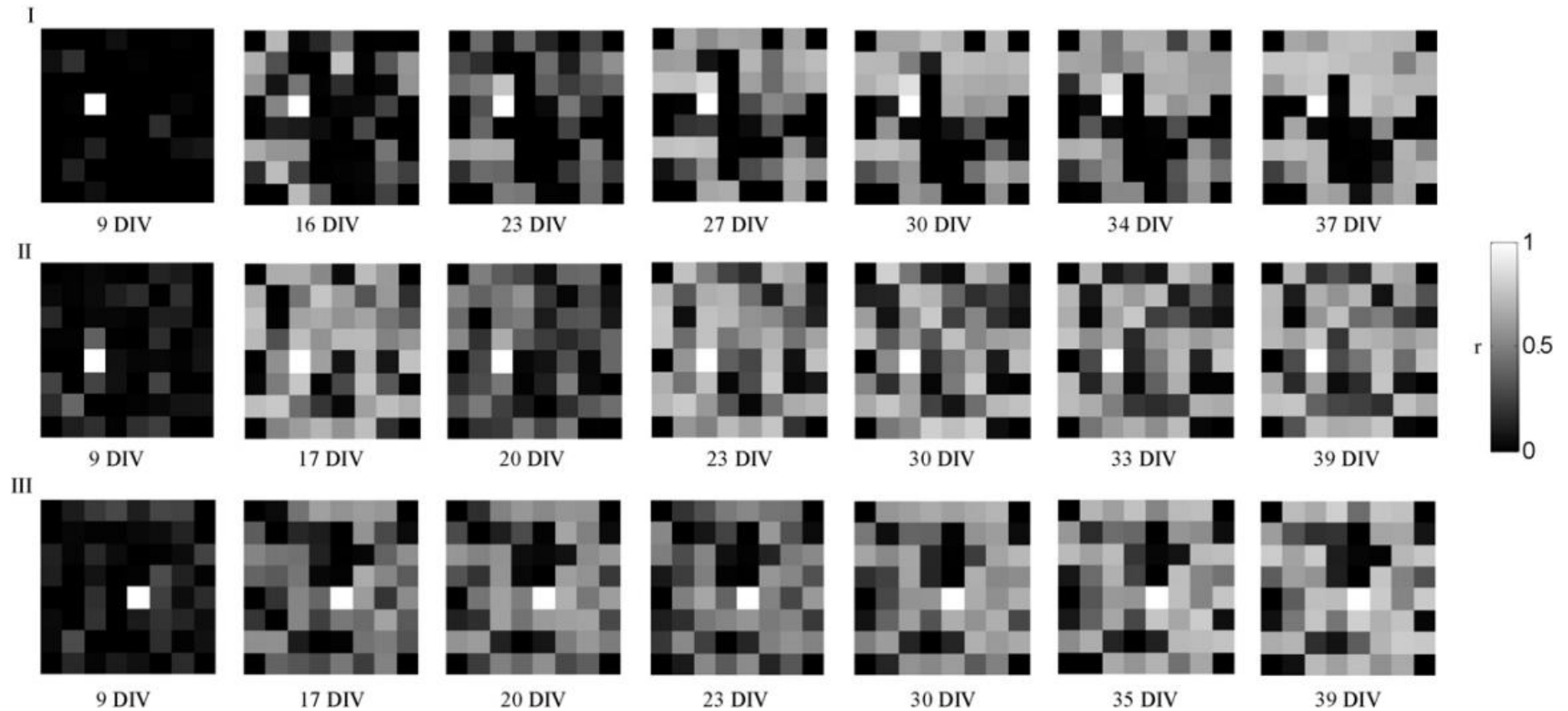


**Figure 2.7:** Gray scale representation of the cross-correlation coefficients ( $r$ ) computed between a reference electrode (indicated as the white color square in each block) and each of other electrodes in three independent cultured networks on different days *in vitro*. The gray scale of each square represents the correlation between the electrode and the reference, with white representing the highest correlation of 1 and black representing zero correlation. Note that the arrangement of the squares in each block represents the position of the 60 electrodes in the MEAs, excluding the four squares at the corners.

## 2.5 Discussion

Conventional drop-seeding technique is effective for preparing high-density cultures from a concentrated cell suspension. The latter can be readily accomplished in freshly dissociated cells by spinning and proportional dilution to the desired plating density. However, centrifugation can deteriorate the quality of cells, especially the cryopreserved neurons which are highly susceptible to mechanical stress (Kawamoto and Barrett 1986). Besides, centrifugation also promotes clumps formation as the unwanted constituents from damaged cells are released into the suspension (Patel et al., 1998). Disaggregating these clumps of neurons by vigorous suspension, in turn, causes significant deterioration to the cells.

We have developed a device to promote high-density seeding of cell suspension with low concentration in MEAs. By incorporating the device during cell seeding, it enables us to increase and control the plating density inside the culture chambers without requiring centrifugation. This can substantially reduce the formation of cell clumps which often poses considerable difficulties in the neural cell cultures. More importantly, the device has allowed us to prepare successful primary cultures from cryopreserved neurons and glia which usually have considerably lower viability than those prepared from freshly dissociated cells.

One major concern about the device is the possible damage incurred to MEAs through its direct physical contact with the fragile electrode tracks.

However, with the use of O-ring seals and proper handling, all the recording sites remain intact after repetitive use. The device can easily be detached from the MEA without interfering with the cultured networks. Additionally, it is relatively easy to fabricate, cost-effective and reliable for long-term use with all the parts autoclavable and re-usable.

In the present study, cortical cells were effectively confined to the electrode area of MEAs, eliminating the need to selectively localize the neurons to the electrodes (Wyart et al., 2005) for optimal recordings. Besides, the high plating density achieved with the aid of the device has also compensated for the deficiencies of control cultures, by improving both their electrophysiological activity and neuronal survival. Further analyses of the extracellular recordings demonstrated that the high-density cultures remained spontaneously active over months, exhibited stable development and similar network characteristics as reported by other researchers (Maeda et al., 1995; Kamioka et al., 1996; Eytan and Marom 2006; Jimbo et al., 2006).

Although the present technique was tested only in cortical neurons, it may be extended for use in other dissociated neural cells that require high-density seeding. Most importantly, this simple and inexpensive method offers an alternative to deal with the complexities when using cryopreserved cells.

## **2.6 Conclusion**

We presented a device that can be used to increase the plating density on MEAs for cell suspension with low viability. This is achieved by constraining the cells in a suspension to settle within the electrode area of the MEAs. The device has enabled us to prepare successful cortical cultures from cryopreserved cells.

## CHAPTER 3

### A MULTI-SITE ELECTRICAL STIMULATOR FOR SUBSTRATE INTEGRATED MULTI-ELECTRODE ARRAYS

One of the main advantages of the MEA technique is its capability of multisite stimulation. Here, we present an electrical stimulator that interfaces with our existing recording system to enable simultaneous recording and stimulation through any of the 60 substrate electrodes on the arrays. Stimulation was fully-automated, with the timing and delivery of the stimulus pulses controlled by an on-board microcontroller. We demonstrate that this stimulator is capable of producing stimuli to reliably evoke action potential responses from neuronal ensembles with minimal interference to the extracellular recording.

#### 3.1 Introduction

The scientific urge to explore the fundamental physiological brain functions has led to the widespread use of MEAs (Thomas et al., 1972; Gross 1979; Pine 1980). One of the main features of this electrophysiological tool is its bi-directional, non-invasive electrode interface, which enables repeated stimulation and recording from a large ensemble of neurons. Electrical stimulation through MEAs has been an integral part of many different experimental designs, including studies on long-term development of functional networks (Bologna et al., 2010), distributed neural processing

(Bakkum et al., 2008), input-output relationships (Novak and Wheeler 1988; DeAngelis et al., 1998), as well as research on learning and plasticity *in vitro* (Jimbo et al., 1999; Shahaf and Marom 2001). To serve the needs, advances have been continuously undertaken in the stimulation systems that were made commercially available to researchers. Many groups have also built their own custom stimulators that suit the requirements of their experimental studies (Regehr et al., 1989; Jimbo et al., 2003; Wagenaar and Potter 2004; Rolston et al., 2009).

In an effort towards understanding the dynamics of functional networks, we, like many others, focused on small neural circuits formed by vertebrate neurons in cultures. While the basic stimulator in our laboratory (STG 1002, MultiChannel Systems) is capable of delivering different types of stimulus pulses to evoke neuronal responses in these cultures through MEA electrodes, it suffers from several drawbacks that make it less than ideal for our study. Firstly, because the stimulation sequences would need to be programmed and downloaded into the system ahead of time, and especially since the system has very limited memory capacity, it is not feasible for relatively sophisticated or long-term stimulus protocols. Secondly, the system does not allow automatic switching between stimulation channels during any given protocol. This prohibited us from using spatially diverse or distributed patterns of stimulation, which were shown to be advantageous in sculpting the population dynamics of cultured networks (Wagenaar et al., 2005b; Chao et al., 2008).

Since upgrading of the stimulation system is extremely costly, and we find it difficult to modify the stimulator without knowledge of its circuit design and application software, we developed our own system. This relatively simple stimulator is to be integrated with our existing recording setup to enable simultaneous recording and stimulation from substrate integrated MEAs *in vitro*. To verify the functionality of the system, we tested it on cultured networks of cortical neurons, and found that it could reliably evoke responses from within the neuronal ensembles.

### **3.2 A Multi-site Electrical Stimulator**

Figure 3.1 shows the circuit design of the electrical stimulator developed in this study. Like many commercial stimulators, our stimulus generation circuit features an on-board microcontroller (PIC18F4620, Microchip) in its design. The stimulator is powered by an external  $\pm 15$  V supply, and controlled through a serial port of a standard desktop computer. It generates timed voltage pulses with both programmable amplitude and timing. Voltage amplitude is set with an 8-bit I/O port of the microcontroller via a digital-to-analog converter (DAC) (TLC7628, Texas Instruments), which in turn drives the operational amplifier (OPA4227, Burr-Brown) to produce stimuli in the range of  $\pm 2.048$  V. The amplitude of the pulses could be specified to 16 mV precision within this selectable range. The timing of the stimulus pulses is controlled via a built-in timer of the microcontroller, which outputs pulses at the desired stimulation time. The width of the pulses is also programmable, with steps of 40  $\mu$ s. These pulses are transferred to the electrodes through a

pair of single-pole cables (terminal “S”) that plugs directly into the preamp (MEA1060-Inv-BC, MultiChannel Systems), which contains a set of isolation switches to allow stimulation of different electrodes.

Instead of storing the entire stimulation sequence on the program stack of the microcontroller, a single stimulus pattern is transmitted from the computer to the microcontroller at a time, and this pattern is renewed shortly before the start of the next stimulus. Stimulation channels are updated with each renewal of the stimulus pattern. A new set of switching signals is routed to the preamp through a separate serial port of the computer (not shown) to program the switches therein whenever a new stimulus pattern arrives. This relieves the microcontroller from having to store a large amount of data, and allows easier switching between different stimulation channels. The switching signals were derived from the protocol of MEA Select software (MultiChannel Systems) to direct stimuli to one or more of the electrodes. Stimuli of the same pattern can be delivered to any number of electrode sites simultaneously, while different stimuli can be applied following a minimum latency of 3 ms. Artifact suppression is performed with the blanking circuitry from the preamp. The circuit is triggered each time upon receiving a blanking signal from the microcontroller (terminal “B”), which is delivered shortly before the start of the stimulus. An example is shown in Figure 3.2. The parameters of the stimulus pulses, their timing, and the selection of stimulation channels are programmed with a graphical user interface developed in Visual C#.



B

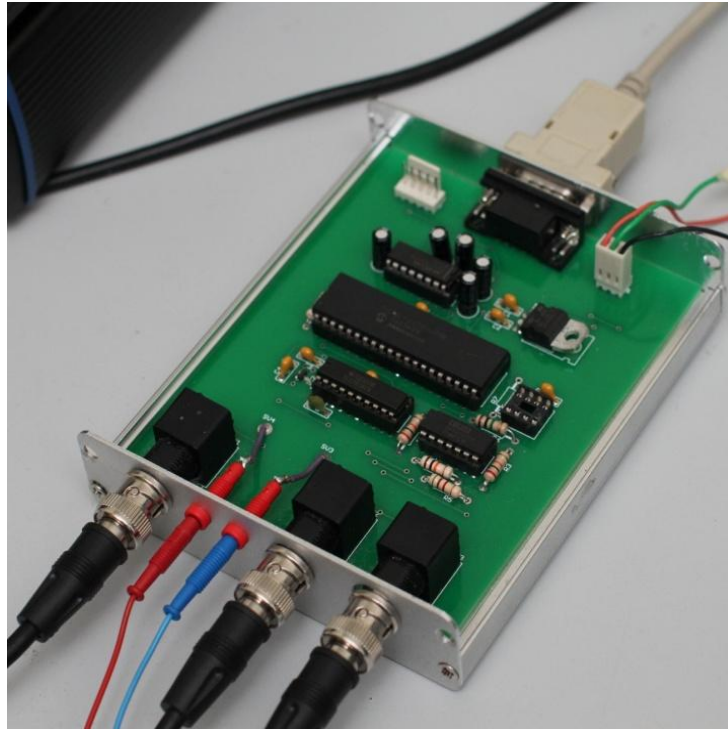


(Figure 3.1, continued)

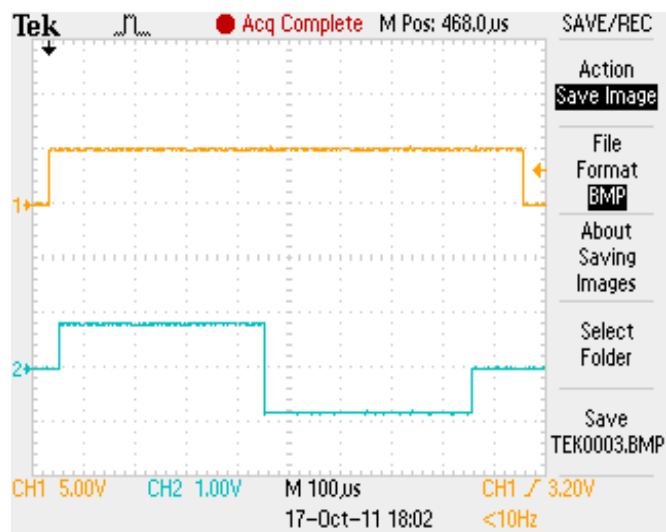


**Figure 3.2:** Screenshot from the oscilloscope showing a blanking (TTL) pulse (top) and a biphasic voltage pulse (bottom). Note that the TTL pulse is delivered 10  $\mu$ s before the stimulus and stops 100  $\mu$ s after the stimulus.

### **3.3 Methods**

#### **3.3.1 Cell Culture**

Neocortex was dissected from E18 rat embryos and cut into pieces of about 1 mm<sup>3</sup>. The extracellular matrix of the tissue was weakened by incubation in 0.25% trypsin at 37 °C, followed by gentle trituration using a sterile 1 ml pipette tip to dissociate the partially digested tissue. The resulting suspension was diluted into 2500 cells/μl with Neurobasal medium (Invitrogen) supplemented with 5% Equine serum (HyClone), 2% B27 (Invitrogen) and 0.05 mM Glutamax (Invitrogen). Cells were then added in drops of 50 μl, on MEAs pretreated with PEI (Sigma). They were allowed to attach onto the substrates for 2 hours before added with another 1 ml of medium. All cultures were sealed with Teflon membranes (Potter and DeMarse 2001) and maintained in an incubator.

#### **3.3.2 Recording**

Electrical activity was recorded from cortical neurons cultured atop the MEAs consisting of 60 titanium nitride electrodes, 30 μm in diameter, embedded in the substrate at 200 μm spacing (MultiChannel Systems, Reutlingen, Germany). After 1100x amplification, signals were sampled at 25 kHz using a data acquisition card (MC Card, MultiChannel Systems). The recorded voltage trace was high-pass filtered at 200 Hz to remove the low-frequency postsynaptic potential components. Spikes were then identified by

thresholding at 5x estimated standard deviation of the background noise. To reduce double detection of spikes with multi-phasic waveforms, candidate spikes of smaller amplitude within a  $\pm 1$  ms window were discarded.

### **3.3.3 Electrical Stimulation**

Electrical stimuli were generated using the circuit depicted in Figure 3.1A. All pulses were less than 900 mV in amplitude to avoid damaging the cells or electrodes. The stimulus pulses were delivered either repeatedly through a single electrode, or consecutively to each of the substrate electrode on the arrays. In all trials, the interval between two consecutive pulses was set to be 2 seconds, a sufficiently long time to allow the networks to recover from the previous stimulus.

## **3.4 Results**

### **3.4.1 Measured Specifications**

This section describes the detailed specifications of several important aspects of the stimulation system, including noise level, artifacts induction and switching precision.

*Noise.* The substrate electrodes on MEAs were evaluated for their noise level in the frequency range of 200-3000 Hz, as was normally used for spike

detection. Without the stimulator, the measured value of RMS noise was  $1.84 \pm 0.03 \mu\text{V}$  (mean  $\pm$  standard deviation;  $N=59$  electrodes). With the stimulator connected to the preamp, the RMS noise was  $1.87 \pm 0.04 \mu\text{V}$ , not much different from the existing platform.

*Switching artifacts.* Switching artifacts were identified as the transients induced shortly before and after a stimulus pulse, during which electrodes were triggered to switch between stimulation and recording. On the non-stimulation electrodes minor artifacts were recorded during the switching events, with the peak amplitude of the artifacts measured to be  $<80 \mu\text{V}$  in close to 100% of the trials (with blanking system enabled). On the stimulation sites such artifacts were often mixed with the stimulus-induced artifacts, leading to large transients beyond the amplifier's dynamic range ( $\pm 819 \mu\text{V}$ ) for tens of milliseconds.

*Switching time.* The timing of switching events was controlled by the hardware settings of the switching devices. The duration for switching between stimulation and recording through the same electrodes was in the range of a few hundred microseconds,  $<500 \mu\text{s}$  on average ( $N=300$ ).

*Stimulation artifacts.* The sizes and duration of the stimulation artifacts varied considerably between trials, depending on electrode impedances as well as stimulus strength. When tested with biphasic pulses of 800 mV and 400  $\mu\text{s}$  per phase, as commonly used for experiments, the signals on the stimulation sites

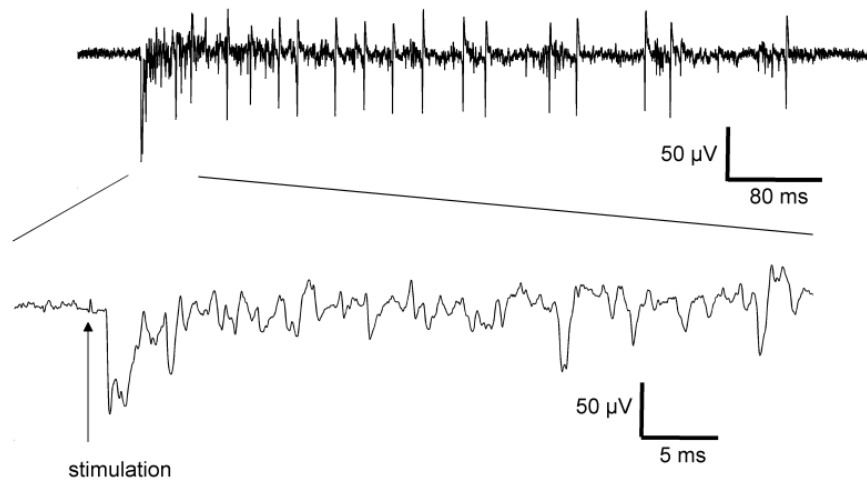


**Figure 3.3:** Evoked response recorded at a non-stimulated site. The stimulus used in this case is a biphasic voltage pulse of  $\pm 500$  mV, 400  $\mu$ s per phase (positive phase first). An expanded view of the beginning part of the response is shown below. The arrow indicates the time of stimulation. Note that spikes were clearly discriminated over that of the baseline noise shortly following the stimulus.

were found to be transiently driven outside the amplifier's dynamic range in all trials, for 60 ms on average ( $N=300$ ). On the other electrodes artifacts lasted only for the duration of the stimulus pulses, and were readily eliminated with the blanking system.

### 3.4.2 Evoking Neuronal Responses with Extracellular Stimuli

The performance of the stimulation system in a few key technical areas has been assessed in the previous section. Yet, it is important to demonstrate that the system could be used to reliably evoke responses in neuronal networks. To evaluate this, we performed stimulation on rat cortical cultures growing on MEAs (see Methods). Cultures used for this test were in the age range of 40-50 days *in vitro* to ensure fully developed synaptic connections. In all cultures tested ( $N=7$ ), stimulation were found to be effective at multiple sites in

eliciting neuronal responses; spikes that were time-locked to the stimulus pulses delivered through different substrate electrodes were consistently observed across trials. An example of evoked response recorded on one electrode following a single biphasic pulse is shown in Figure 3.3.

To better illustrate the reliability and timing of the stimulus responses, an array-wide raster plot of spikes recorded following stimulation on a single electrode for 20 consecutive trials is presented (Figure 3.4). It clearly revealed evoked responses that diffusely spread in time on the vast majority of the electrodes across most trials, implying that the induced excitation did spread appreciably throughout the entire network.

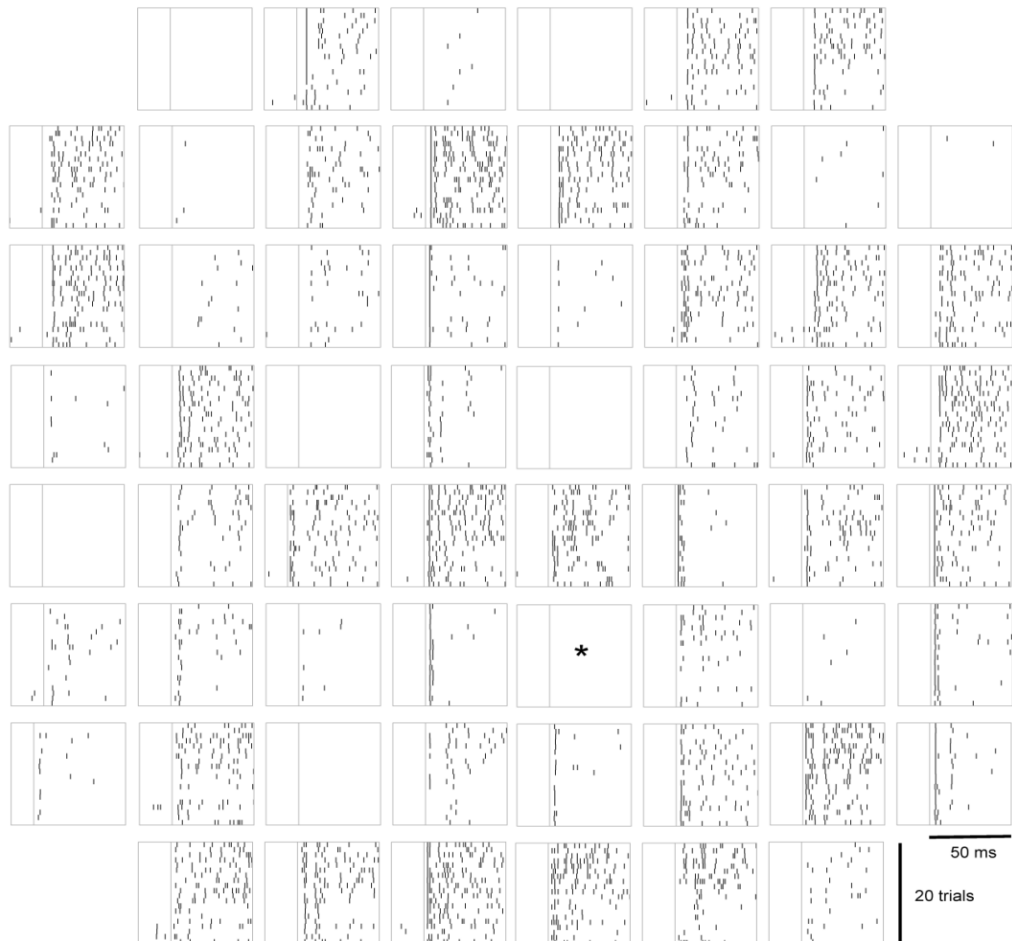


**Figure 3.4:** Raster plot showing the array-wide responses following stimulation on a single electrode for 20 trials. The 8x8 layout matches the physical geometry of the MEAs. Constant voltage stimuli of  $\pm 700$  mV and 400  $\mu$ s were used in this case, delivered through the electrode marked by ‘\*’. Vertical lines denote the timing of stimuli. Consecutive trials are stacked along the vertical axis, while the horizontal axis marks the time at which a spike was detected. Spikes on all electrodes, except the one used for stimulation, were detected following a 4 ms latency after the stimulus pulses.

### 3.5 Discussion

We present an electrical stimulator that interfaces with the MEA1060-Inv-BC preamp to enable stimulation through any of the 60 electrodes on the MEAs. This stimulator meets both our design objectives: (1) it improves on the permitted length of stimulus sequences and (2) it enables flexible switching between stimulation channels. Such improvements on available commercial stimulation systems have granted us greater flexibility in designing our stimulus protocols, including spatio-temporal distributed patterns of stimulation that were not possible before. Although the stimulator was designed to produce voltage-controlled stimuli, it could be readily adapted to allow current-controlled stimulation by adding a voltage-to-current converter circuit. Furthermore, the stimulator could also be improved to handle more complicated pulse shapes by replacing the DAC with a higher resolution one that allows generation of stimulus waveforms over a wider dynamic range.

The stimulator is capable of producing stimuli to reliably evoke action potential responses from neuronal ensembles with minimal interference to the extracellular recording. We have used it to elicit spiking responses from dissociated cortical cultures, and were able to reduce the stimulus artifacts using the built-in blanking system of the preamp. However, with this approach, any spikes that occurred within the duration of blanking were lost. This made our stimulation system less ideal for studies where very early latency responses are critical. Improvements could be made on the hardware, for example, by using the sample-and-hold technology which permits rapid

recovery from stimulus artifacts on all electrodes, including those used for stimulation (Novak and Wheeler 1988; Jimbo et al., 2003). Alternatively, software solutions to artifact suppression could also be employed. An example of such algorithm is SALPA (Wagenaar and Potter 2002), which had been shown to perform well on a wide range of artifact shapes.

One of the most attractive advantages of *in vitro* networks is probably its non-invasiveness, which enables easy manipulation of the neuronal activity with various external stimuli. Using this multi-site stimulator, we could study how different types of controlled artificial inputs affect the structure and activity of cultured networks by probing them with the desired stimulus patterns. Additionally, since parallel stimulation could be performed through multiple sites of the networks, the use of this stimulator thus enables a high number of stimulus-response combinations to be addressed. Combining this stimulator with the extracellular recording would serve as a useful platform for understanding the spatio-temporal information processing in neuronal networks, as well as the activity-dependent dynamics of these cultures.

## CHAPTER 4

### ULTRA-SLOW OSCILLATIONS<sup>†</sup>

An ultra-slow oscillation ( $<0.01$  Hz) in the network-wide activity of dissociated cortical networks is described in this chapter. This slow rhythm is characterized by the recurrence of clusters of large synchronized bursts of activity lasting approximately 1–3 min, separated by an almost equivalent interval of relatively smaller bursts. Such rhythmic activity was detected in cultures starting from the fourth week *in vitro*. Our analysis revealed that the propagation motifs of constituent bursts were strongly conserved across multiple oscillation cycles, and these motifs were more consistent at the electrode level compared with the neuronal level.

#### 4.1 Introduction

Large-scale rhythmic oscillation is the hallmark of brain physiology and is believed to underlie diverse processes of the nervous system. The frequency of electroencephalographic oscillation encompasses a multitude of frequency bands that varied with the functional state of the brain. Slow rhythm ( $<4$  Hz) is particularly crucial in deep sleep stages, where it has been detected over widespread regions in the thalamocortical networks. The broad range of the slow rhythm belongs to at least three different types of oscillatory activities

---

<sup>†</sup> Published as: S. Y. Mok, Z. Nadasdy, Y. M. Lim, and S. Y. Goh, 2012: Ultra-slow oscillations in cortical networks *in vitro*. *Neuroscience*. **206**, pp. 17-24.

with each playing potentially different roles, including delta rhythm ranging from 1 to 4 Hz (Steriade et al., 1993a,b), slow oscillation with frequency of 0.01 to 1 Hz (Metherate and Ashe 1993; Steriade et al., 1993a,b; Contreras et al., 1996; Achermann and Borbély 1997), and ultra-slow oscillatory activity that recurred on the order of 0.001–0.01 Hz (Penttonen et al., 1999; Vanhatalo et al., 2004; Drew et al., 2008).

Although the slow rhythm was once thought to arise only within local networks *in vivo*, there is compelling evidence that slow network oscillations could be expressed *in vitro* (Timofeev et al., 2000). The study of this recurrent activity in *in vitro* networks is potentially useful, as it leads to a better understanding of the slow rhythm in intact brains. Previous experiments with cortico-thalamic slices have provided important insights on the cellular and network mechanisms that may account for the generation of slow rhythm (Sanchez-Vives and McCormick 2000; Hughes et al., 2002; Shu et al., 2003; Lőrincz et al., 2009), as well as the effect of varying the temperature of bath solution on cortical rhythms (Reig et al., 2010). However, slow network oscillations on the time scale of minutes have not been shown in dissociated cortical culture that is lacking of the specific cytoarchitecture *in vivo*.

Here, we demonstrate the spontaneous emergence of a very slow network oscillation (<0.01 Hz), hereafter termed ultra-slow oscillation, in dissociated cortical networks in culture. Our results indicate that the propensity of this rhythmic activity was enhanced with the application of low-frequency electrical stimulation. We also found repeating motifs of bursts in the ultra-

slow oscillations, based on the analysis of their propagation profiles during burst initiation.

## **4.2 Experimental Procedures**

### **4.2.1 Cell Culture**

Embryos were obtained from timed-pregnant Wistar rats euthanized using CO<sub>2</sub> at day 18 of gestation. The cortices were dissected and cut into small pieces in ice-cold Hanks' balanced salt solution (Invitrogen, Carlsbad, CA, USA). This is followed by enzymatic digestion by incubation in 0.25% trypsin (Invitrogen) at 37 °C for 15 min. The partially digested tissues were mechanically triturated using 1 ml pipette tips and centrifuged at 150xg for 6 min. The cells were fully dissociated by gentle trituration and diluted into 2500 cells/μl in Neurobasal medium (Invitrogen) supplemented with 5% Equine serum (HyClone, Logan, UT, USA), 2% B27 (Invitrogen), and 0.05 mM Glutamax (Invitrogen). Before plating, we mixed the cell suspension with 1 mg/ml laminin (Sigma, St. Louis, MO, USA). Subsequently, 50 μl of cells were deposited onto the central region of each MEA, which was pre-coated with PEI (Sigma). The cells were allowed to attach onto the substrates for 2 h, before being flooded with 1 ml of medium. The cultures were sealed with Teflon membranes (Potter and DeMarse 2001) and kept inside the incubator. Half of the medium was replaced every 4-6 days.

#### 4.2.2 Electrical Recording and Stimulation

Cortical neurons were cultured on MEAs (MultiChannel Systems, Reutlingen, Germany) with 60 titanium nitride electrodes, 30  $\mu\text{m}$  in diameter, laid out on an 8x8 grid with 200  $\mu\text{m}$  inter-electrode spacing. Electrical activity from the cultures was amplified 1100x using a commercial 60-channel amplifier (MEA1060-Inv-BC, MultiChannel Systems) with frequency limits of 10 Hz to 3 kHz. Signals were sampled at 25 kHz at 14-bit resolution using a data acquisition card (MC Card, MultiChannel Systems). Online visualization was performed with MC Rack software (MultiChannel Systems), whereas spike detection and the subsequent data analysis were performed using Matlab (MathWorks).

Cultures were probed with biphasic voltage pulses of  $\pm 800$  mV, 400  $\mu\text{s}$  per phase (positive phase first) twice a week starting from the first week *in vitro* using a custom-made stimulator. The stimuli were applied sequentially at 3 s intervals through eight electrodes in the fifth column of MEAs, for a total duration of 3.5 h. In all experiments, spontaneous activity was recorded immediately before and after the stimulation. For the purpose of comparison with non-chronically stimulated (control) cultures, we also monitored the activity of the latter group before and after the application of the same stimulus for 3.5 h. Experiments on the control group were performed using new culture each time, to prevent any unintentional effect which might be caused by earlier stimulation.

All experiments were performed inside the same incubator used for maintaining cultures. To stabilize the temperature of the MEA substrates, excess heat from the amplifier was dissipated with our custom-made heat exchanger. Experiments were started 30-40 min after transferring the cultures to the amplifier. We scheduled all our experiments at least 12 h after feeding to avoid electrophysiological transients (Potter and DeMarse 2001; Wagenaar et al., 2006b).

### 4.2.3 Spike Detection and Sorting

The voltage traces were first high-pass filtered at 200 Hz to remove the low-frequency postsynaptic potential components, yielding a flat baseline. Spikes were then detected by thresholding at 7.5x estimated standard deviation of the background noise<sup>‡</sup> (Quiroga et al., 2004). Subsequently, candidate spikes of smaller amplitude within a  $\pm 1$  ms window were discarded, to prevent duplicate detection of multi-phasic spikes (Wagenaar et al., 2005a).

Single-unit activity was isolated by spike sorting. We used a modified version of WaveClus (Quiroga et al., 2004), in which we applied the discrete derivative method for feature extraction (Nadasdy et al., 2002; Gibson et al., 2010) and superparamagnetic clustering for clustering the feature space. Up to four single units were isolated from each electrode. Single units were validated by a 3 ms refractoriness test. Spike times were resampled at 1 ms.

---

<sup>‡</sup> This threshold was selected as it worked well for the single-unit data analysis, by greatly reducing the number of low amplitude “noise” spikes in the data.

#### **4.2.4 Burst Detection**

Bursts were identified according to a method previously described (Wagenaar et al., 2005a). We first extracted sequences of at least four densely spaced spikes with a maximum ISI of 100 ms as the core of bursts on individual electrodes. They were later extended to include the entourage of spikes on the same electrodes with ISIs less than 200 ms. A network burst is then defined as an episode of temporally overlapping burst activities spanning five or more electrodes over the entire array.

#### **4.2.5 Periodicity**

To better examine and illustrate the periodicity of the network activity, fast Fourier transform (FFT) analysis was performed on population firing rate obtained with a bin width of 4 ms. Before FFT, the DC component was removed by subtracting the mean from the data. The analyses often yielded more than one dominant frequency over the spectrum of interest, as the intervals between successive bursts varied slightly from one another. For this reason, the oscillation frequency is defined as the highest peak within the frequency band of 0-0.01 Hz.

#### **4.2.6 Similarity Indices**

A burst similarity index ( $S_{burst}$ ) was computed based on the method described in Raichman and Ben-Jacob (2008). For each burst, we searched for the first

spikes on all the active electrodes. The latency between electrode pair  $(i, j)$  during the initiation of burst  $n$ ,  $t_n(i, j)$ , was obtained by calculating the relative difference in the timings of their first spikes. The similarity index between burst  $n$  and  $m$  was then defined as the fraction of electrode pairs with the difference in their latencies between the two bursts less than a prespecified threshold,  $t_c$ :

$$S_{burst}(n, m) = \frac{1}{N(N-1)} \sum_{i \neq j} H(t_c - |t_n(i, j) - t_m(i, j)|),$$

where  $H$  is the Heaviside-step function and  $N$  is the number of active electrodes.

The calculation was repeated using neuron pairs  $(i, j)$  obtained from spike sorting. Only neurons with mean firing rate of at least 0.5 spikes per second were included in the analysis. We set  $t_c = 0.03$  seconds (Raichman and Ben-Jacob 2008) in both analyses at the electrode and neuronal level.

### 4.3 Results

Extracellular recordings revealed the spontaneous emergence of ultra-slow oscillations in the network-wide aggregate firing rates of chronically stimulated and control cultures during the fourth to sixth week *in vitro*. In both groups of cultures, an increased propensity of such rhythmic patterns was detected in the network activity after probing the cultures with low-frequency electrical pulses (see Experimental Procedures). This slow rhythm was detected in four recordings before stimulation and in eight recordings after

stimulation out of the total 20 recordings made from chronically stimulated cultures ( $n = 5$  cultures). In control cultures, the rhythmic activity was exhibited in three and five separate cultures out of 13 cultures before and after stimulus delivery, respectively. This slow periodicity persisted with high fidelity over hours once it has developed in the culture, regardless of whether the latter was exposed to chronic stimulation.

The ultra-slow oscillations were shown as a succession of up and down states at frequencies of 0.002-0.008 Hz. The aggregate firing rates at peaks were on average 2-4 times higher than at troughs, with the majority of the spikes contained in bursts of different sizes (Figure 4.1A). The oscillation frequency of such sequences was manifested as a prominent peak in the power spectral density (Figure 4.1B). Bursts were separated by intervals of 2–5 s, and longer IBIs preceded bursts with higher number of spikes (Figure 4.1C), implying that burst sizes were determined by parameters recovered from previous bursts. At neuronal level, the total number of cells contributing to a burst steadily increased with the increase of burst sizes toward the peaks, then leveled off. The average number of spikes per neuron also similarly varied when transitioning from the troughs to the peaks of the oscillations (Figure 4.1D).

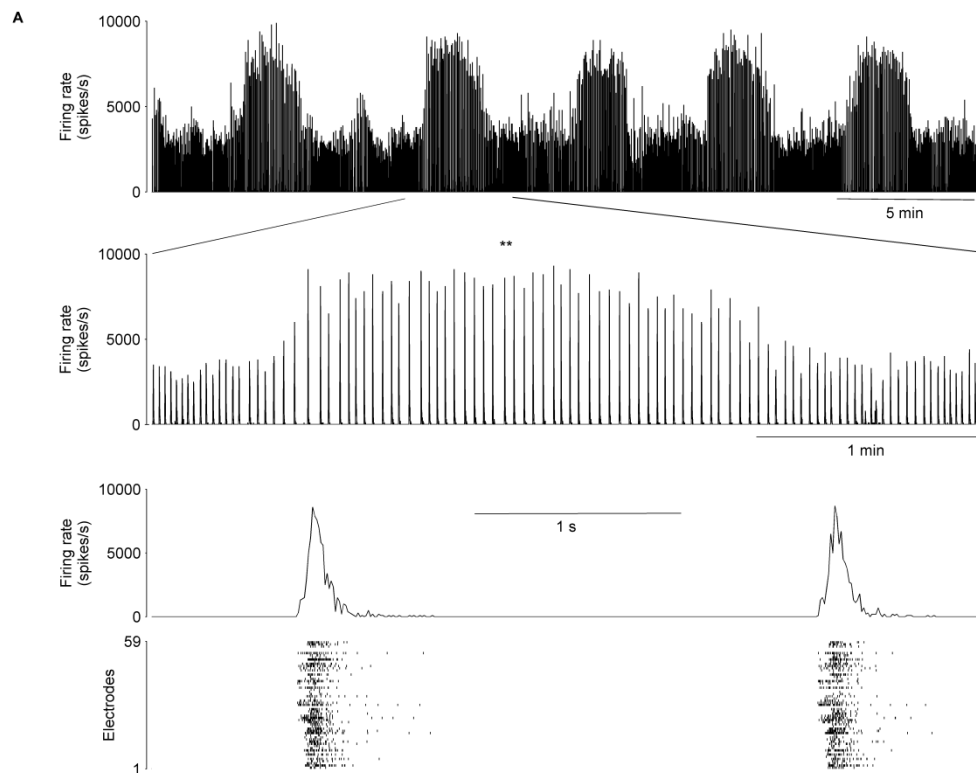


**Figure 4.1:** Ultra-slow oscillations in cortical cultures. A. An example of a 30-min data segment of a 27-d-old cortical culture illustrating the typical ultra-slow oscillations in the network-wide aggregate firing rates. Inset below shows the aggregate firing rates and the simultaneous raster plot of a pair of consecutive bursts (marked by asterisks). The raster plot demonstrates highly synchronized spiking activity among multiple recording sites during the bursting events. B. The corresponding power spectral density of the network activity reveals a prominent peak at 0.003 Hz. C. Variation of burst sizes against preceding IBIs. Dots represent measurements from individual bursts. D. Number of active neurons in bursts (top) and average number of spikes per neuron (bottom) against preceding IBIs.

(continued on next page)

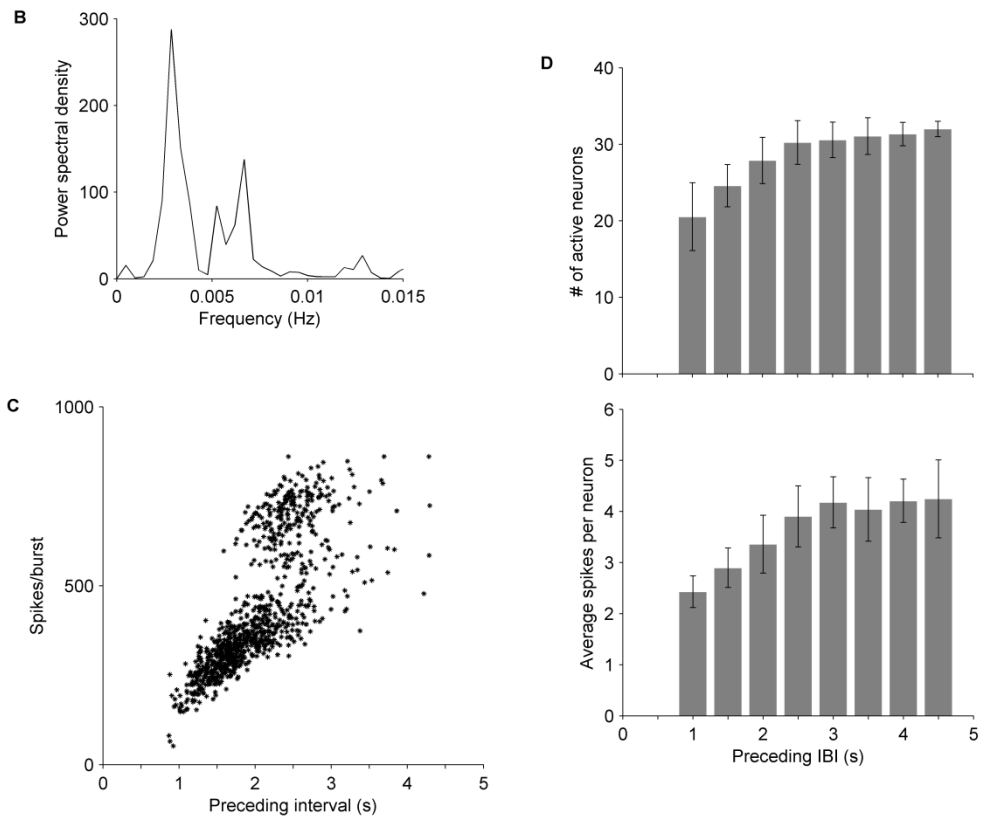


(Figure 4.1, continued)

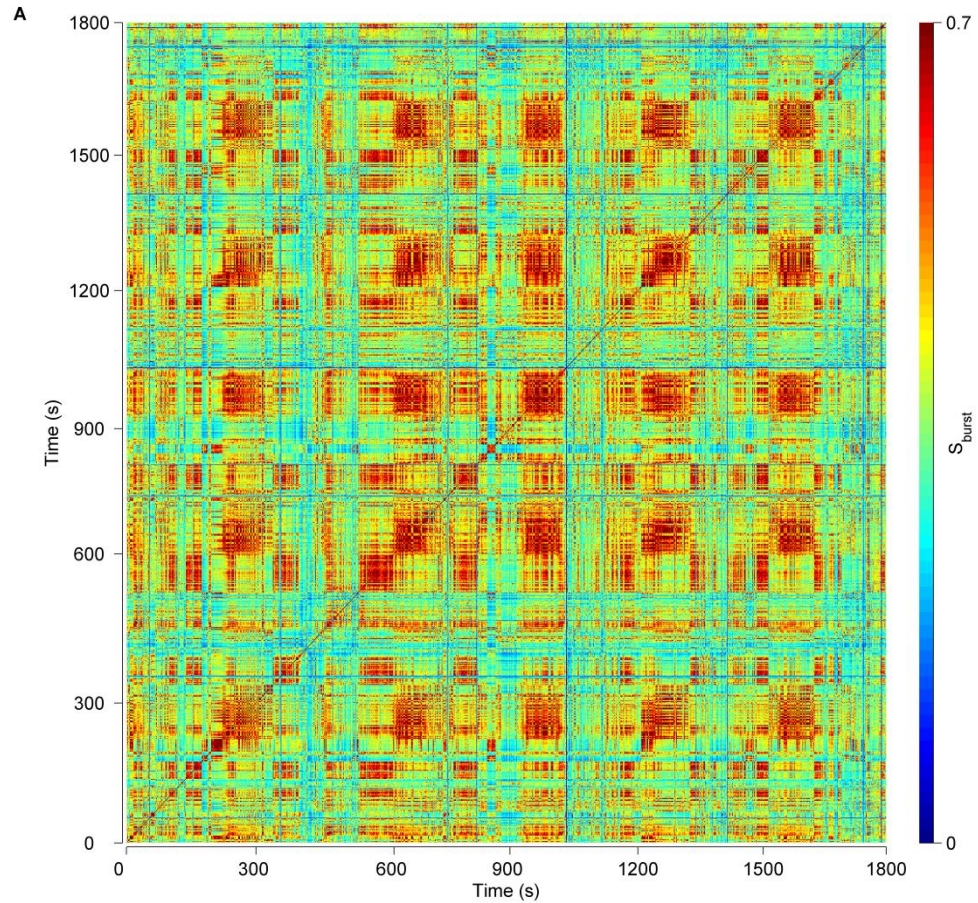


**Figure 4.2:** Identifying burst motifs in the multi-unit activity. A. Similarity matrix between constituent bursts over five consecutive oscillation cycles shown in Figure 4.1A. The peaks were readily distinguished from troughs given the relative difference in their similarities. B. The same matrix shown in A, but rearranged from time order into order of least distance in the correlation space using dendrogram algorithm. The clear block organization in the reordered matrix suggests the presence of distinct subgroups of bursts. C. Distributions of bursts from five different blocks marked by “j” in B. The temporal location of bursts from each block is assigned a different color. D. Raster plot of the temporal locations of bursts from five different blocks, color coded as in C, for two consecutive cycles. Bursts from the same blocks are shown to be expressed in a non-uniform temporal order across the ultra-slow oscillations.

(continued on next page)

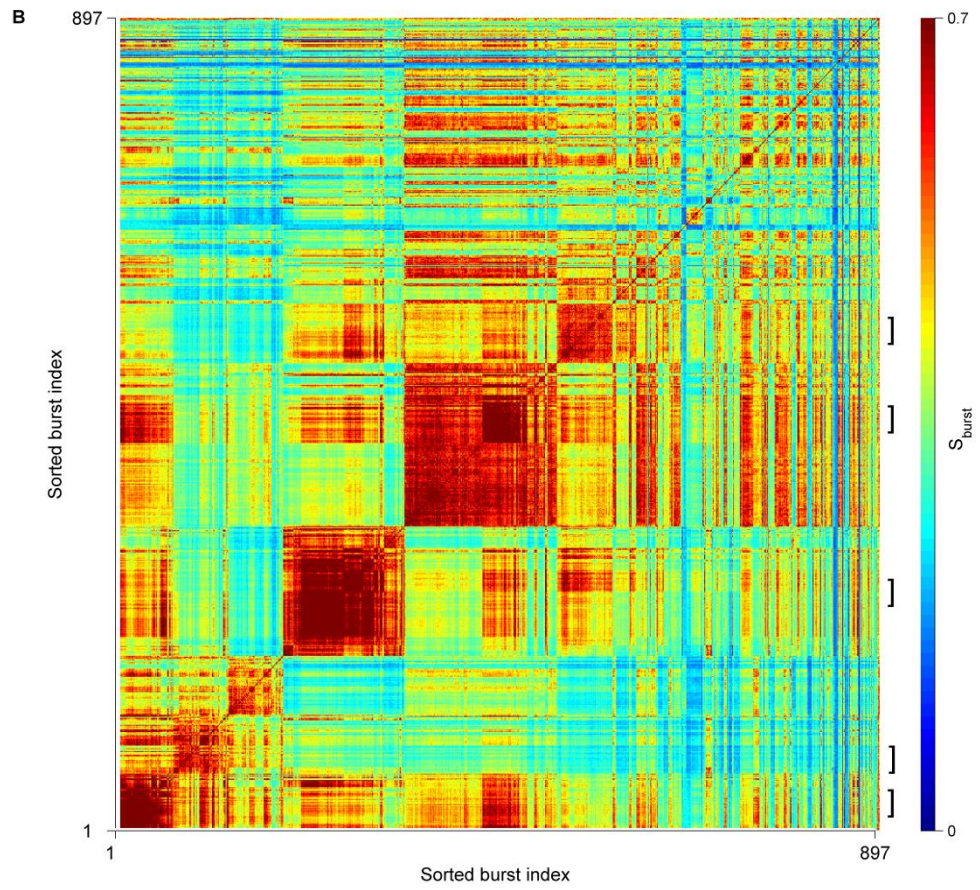


(Figure 4.2, continued)

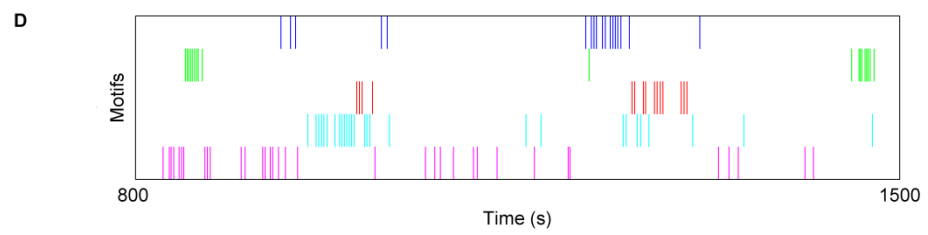
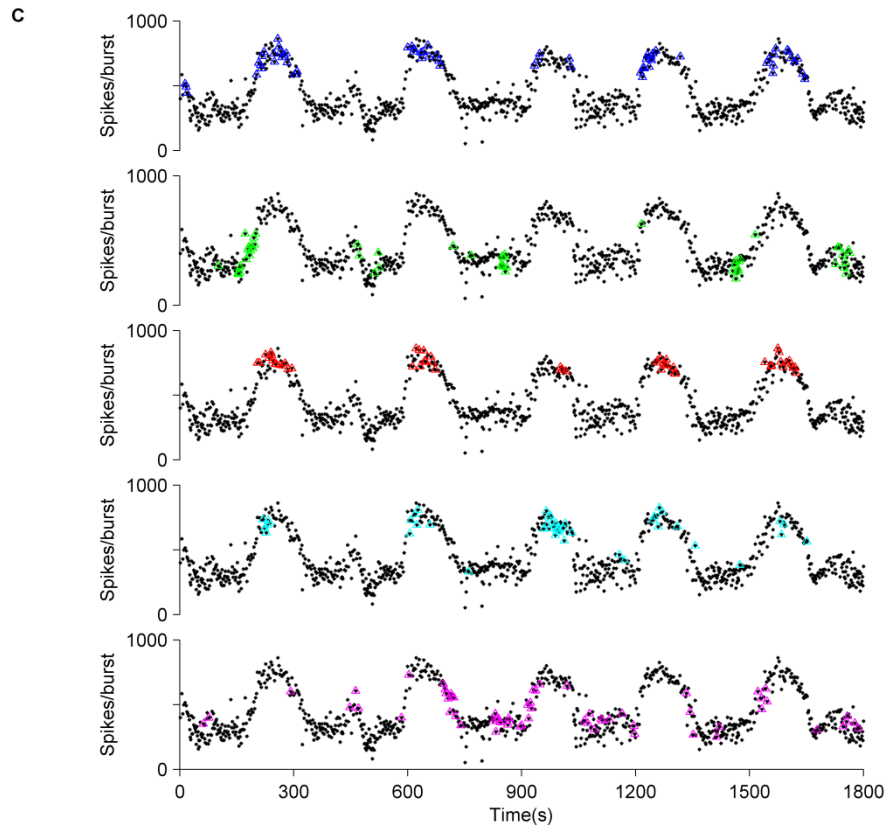


(Figure 4.2, continued)

To investigate whether the spatiotemporal dynamics of activity was conserved across the constituent bursts, an analysis was performed to quantify the similarity in their propagation profiles based on the latencies between individual electrodes during burst initiation (see Experimental Procedures). The similarity index was found to be especially high between bursts at peaks, but was on average much lower between constituent bursts at troughs (Figure 4.2A). To identify clusters of bursts with similar propagation profiles, we reordered the similarity matrix by a standard dendrogram clustering method (Press et al., 1992). In many cases, the sorted matrices exhibited a clear block organization along the diagonal (Figure 4.2B), suggesting the presence of distinct subgroups of bursts with strongly conserved similarity (Segev et al., 2004). Bursts from the same clusters were distributed across successive oscillation cycles separated many minutes apart (Figure 4.2C), indicating that changes in the burst propagation profiles did not occur in discrete time steps. Constituent bursts at peaks and troughs were clustered into separate blocks albeit having a non-uniform temporal order of appearance (Figure 4.2D).

We proceeded to examine the spatial propagation of bursts throughout the networks, by sorting individual electrodes according to the timings of their first spikes in the bursts. The analysis revealed that each cluster of bursts was associated with its own unique motif of propagation, and that the motif was highly repetitive among the component bursts from the same clusters (Figure 4.3). Remarkably, instead of propagating through widely dispersed paths, the burst activity spread through ensembles of neurons on closely spaced

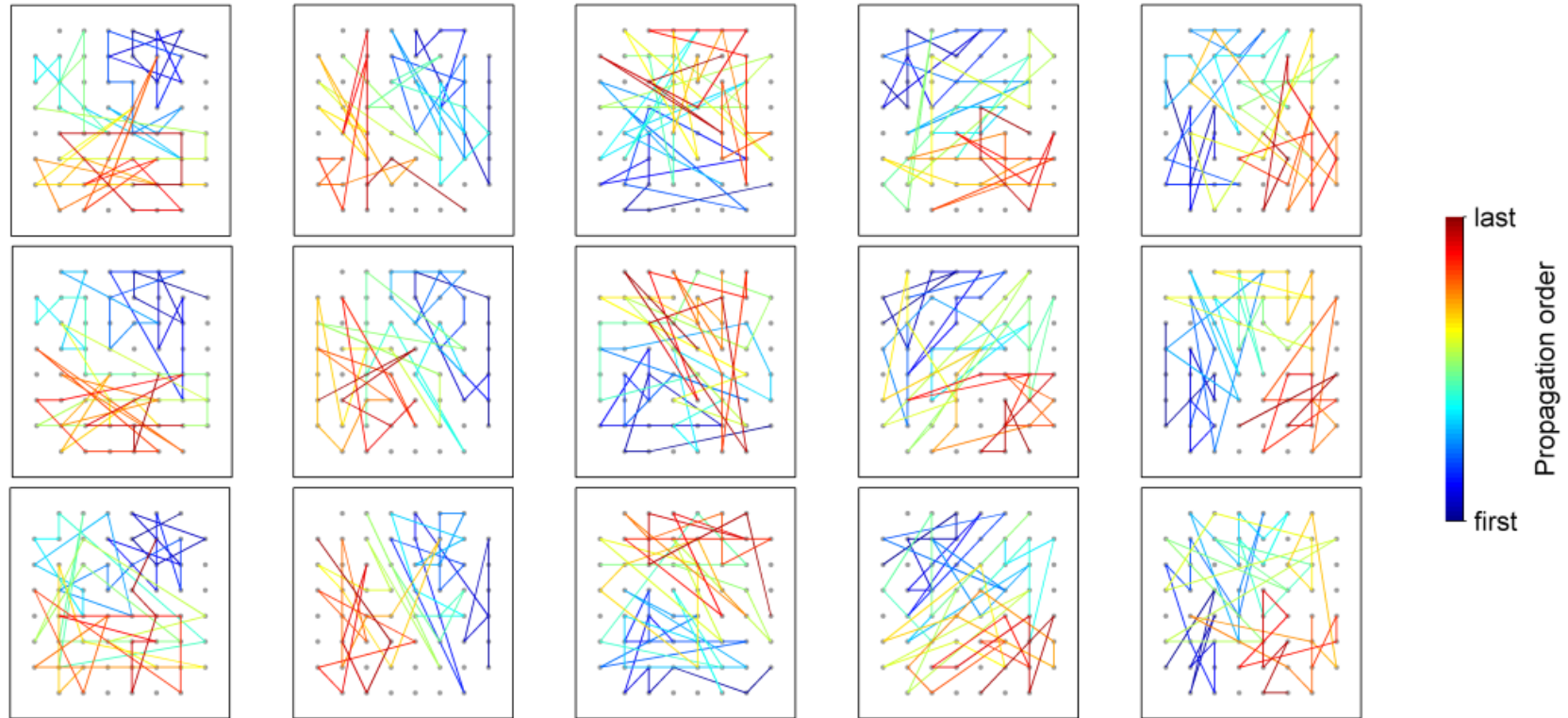


**Figure 4.3:** Distinct spatiotemporal patterns of burst propagation. Each panel displays the activity propagation of an individual burst over the electrode grid, with bursts from each column (left to right) pooled from the same blocks marked by “J” in the similarity matrix (Figure 4.2B; left to right). The lines represent the propagation trajectories of the bursts through the networks, color coded according to the bar at right. Note the consistency in the propagation patterns of bursts from the same block. The panels are laid out following the physical geometry of MEAs.

electrodes. This ordered pattern of burst propagation was most noticeable during a tight series of large bursts with relatively smaller IBIs, as was often observed at the peaks of the oscillations.

To determine the presence of similar motif repetition at neuronal level, we repeated the analysis using single-unit activity obtained from spike sorting. Like the multi-unit activity, the similarity index was much higher between bursts at peaks than the bursts at troughs (Figure 4.4A). However, the level of similarity between bursts was in general lower compared with the multi-unit activity, indicating that the profiles of burst propagation were more consistent at the electrode level. The reduced consistency was indeed evident in the reordered similarity matrix, which showed an increased variance of propagation motifs of bursts (Figure 4.4B).

By sorting the temporal order of individual neurons according to the timings of their first spikes in the bursts, we found that the sequence of neuronal activation was likewise repeatable among component bursts from the same motifs (Figure 4.4C). To better elucidate the conservation in the sequence of neuronal activation, we constructed return plots of burst onset latency (Wagenaar et al., 2006a) for a pair of neurons, measured as the relative delays between the selected neurons and the first neuron recruited in the burst. The return plots showed that individual neurons played conserved roles in component bursts from the same motif; the same neuron that was consistently bursting earlier than another neuron in one motif was bursting later in another motif in a consistent manner (Figure 4.4D).

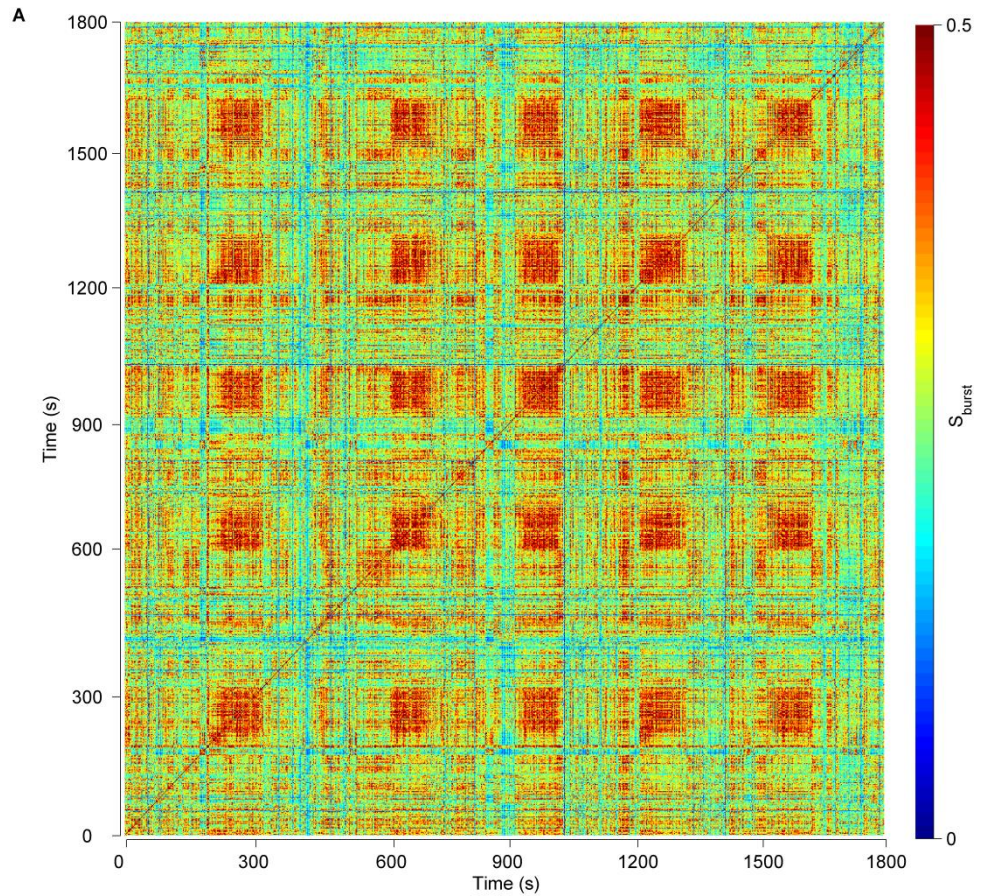


**Figure 4.4:** Identifying burst motifs in the single-unit activity. A. The same matrix shown in Figure 4.2A, but instead of comparing the similarity of bursts based on the latency of first spikes between individual electrodes, the similarity index was computed by comparing the relative difference in the latencies of first spikes between single neurons. B. The reordered similarity matrix. The appearance of block-diagonal structure in this sorted matrix indicates the presence of repeating motifs in the single-unit activity. C. Raster plots of bursts from two motifs in B, with three bursts from each horizontally stacked side-by-side. The black symbols marked the timings of the first spikes on individual neurons during bursts. Insets show the propagation trajectories of bursts over the electrode grid. Note the similarity in the sequence of neuronal activation in bursts from the same motifs. D. Return plots of burst onset latency for two neurons (#1 and #24) from the two motifs shown in C. The red neuron was consistently bursting earlier than the blue neuron in one motif, but the sequence was altered in the other motif.

(continued on next page)

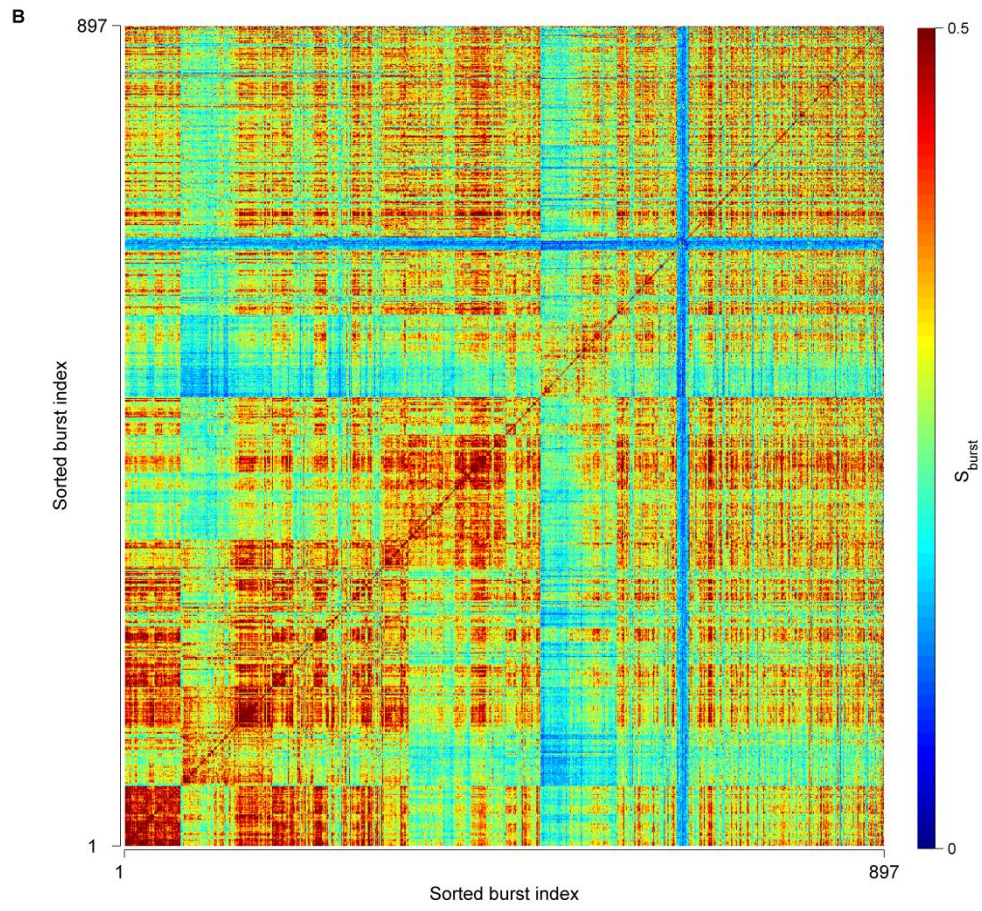


(Figure 4.4, continued)

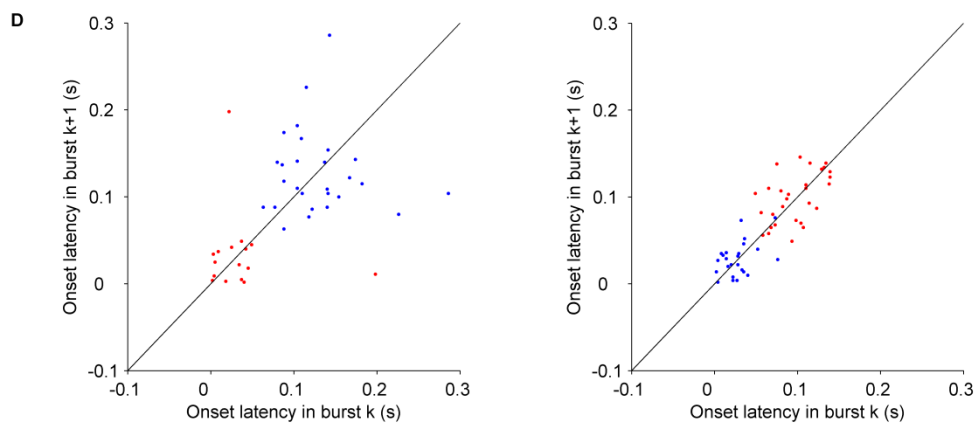
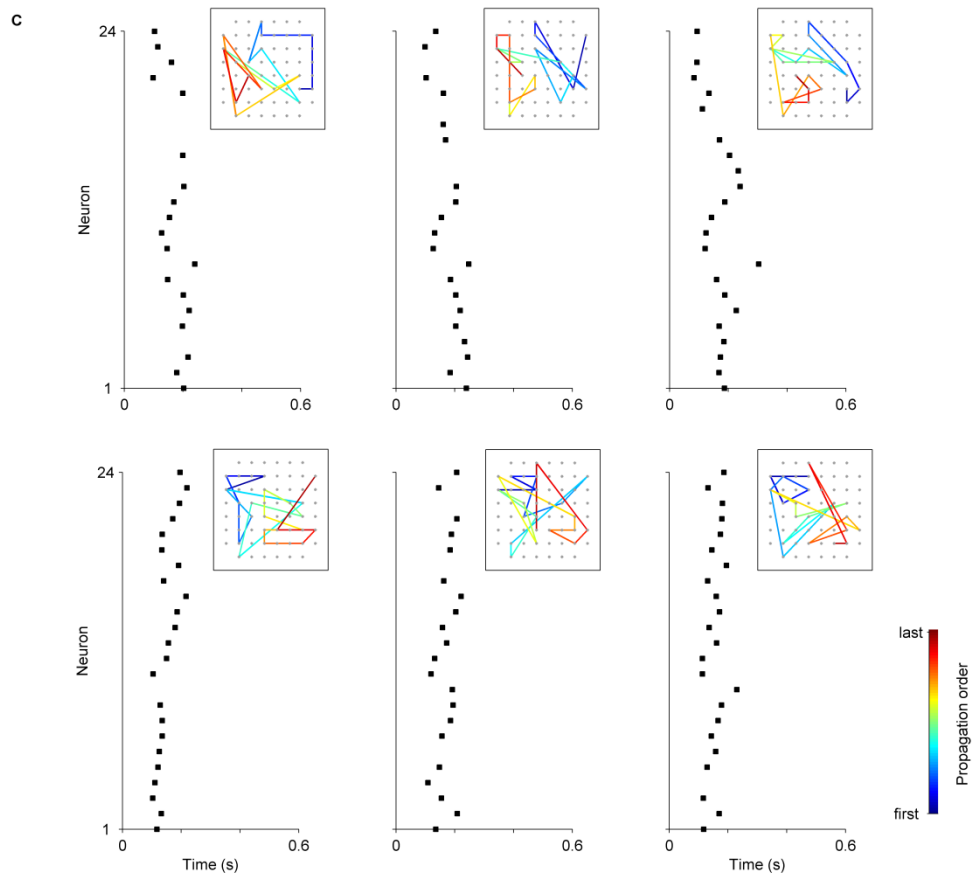


(Figure 4.4, continued)

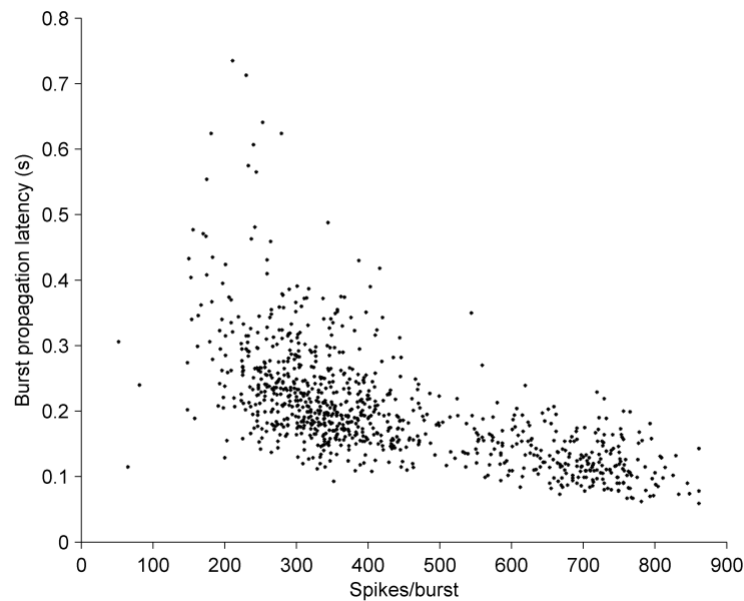


**Figure 4.5:** Burst propagation latency as a function of burst size. Each dot represents a measurement from an individual burst.

The large discrepancy in the similarity level between bursts at peaks and troughs suggests that the duration of burst onset might vary during different phases of the oscillations. To examine whether the latency of burst propagation was conserved across constituent bursts, we measured the relative time delays between the first spikes of the first and the last electrodes recruited in each burst. The burst propagation latency decreased exponentially with an increased number of spikes in bursts (Figure 4.5), indicating that the onset of bursts across electrodes was more tightly synchronized in time during the peaks of the oscillations. This also demonstrates that a larger population of active neurons would find a faster sequence of firing for the same motif to play out itself.

#### 4.4 Discussion

This is, to our knowledge, the first description of ultra-slow oscillations in the network-wide aggregate firing rates of cortical cultures. Recurring periodic activity has been described earlier in dissociated cortical networks, in terms of intracellular calcium transients, or episodes of synchronized bursts (Robinson et al., 1993; Maeda et al., 1995; Gross et al., 2000; Opitz et al., 2002; van Pelt et al., 2005). However, oscillations coordinated across a large population of cortical neurons in culture on the time scale of minutes have not been reported. Such sequences were dominated by network bursts of varying sizes, resembling the oscillations found in the hippocampal cultures at similar culture ages (Zhu et al., 2010). Notably, the frequency of this slow periodicity was also comparable with that of the ultra-slow oscillatory activity observed in the human cortex *in vivo* (Vanhatalo et al., 2004; Drew et al., 2008).

The spontaneous occurrence of these ultra-slow oscillations implies that cortical neurons retained the ability to self-organize in dissociated networks. Thus, no specific developmentally imposed cytoarchitecture is necessary to generate the ultra-slow oscillations. However, the frequency at which this potential manifests itself in a synchronized periodic activity may be fine tuned by the architectural constraints of the network, depending on whether it is a dissociated culture, *in vitro* slice preparation or *in vivo* cortical column. The frequency of a network-wide oscillation is probably dependent on the number of recurrent synaptic connections within the network, the average synaptic delay, and the number of neurons in the network; factors yet to be investigated.

In earlier experiments, slow brain stimulation had been shown to enhance endogenous EEG slow oscillatory activity in healthy humans (Marshall et al., 2006; Kirov et al., 2009). Meanwhile, low-frequency stimulation was also found to be effective in regulating slow oscillations in hippocampal cultures by consistently inducing the “up” states of the oscillatory activity prematurely (Zhu et al., 2010). The activity patterns in our cortical cultures were likewise regulated with the application of low-frequency stimulation, with an increased emergence of ultra-slow oscillations detected in the network activity after the stimulation sessions. However, the propensity of oscillations remained relatively unchanged in the chronically stimulated cultures compared with the control cultures, suggesting that the chronic stimulation had not caused major long-term plastic effects to the networks.

Several studies have demonstrated the identification of repeating spatiotemporal motifs in the spontaneous bursts recorded from cortical networks cultivated on MEAs (Segev et al., 2004; Madhavan et al., 2007; Raichman and Ben-Jacob 2008). In a separate work by Wagenaar et al. (2006a), they found that the spatiotemporal patterns of activity were highly repetitive in subbursts at the same ordinal position of “superbursts” that arose spontaneously in cortical cultures, and these were discussed in terms of attractor dynamics. We similarly found conservation of spatiotemporal substructures of bursts in the ultra-slow oscillations, and revealed that the bursts at peaks and troughs were associated with different motifs of propagation. This implies that constituent bursts at peaks and troughs were transmitted across the networks through their respective paths each time; thus,

we concluded that the architecture of network connectivity formed the basis for these emergent oscillatory activities. Interestingly, stereotyped sequences of spiking activity were also manifested in the slow oscillations that recurred on a much longer time scale in cortical populations *in vivo* (Luczak et al., 2007). Unlike the repeating propagation motifs of bursts alluded previously in our cortical cultures, however, the activity sequences for the cortical populations *in vivo* were computed from spike latencies of individual neurons relative to the onset of the “up” states.

We also compared the difference of the motif repetition between multi-unit activity and single-unit activity, and found that the propagation motifs of bursts were less consistent at the neuronal level. The increased variance in neuronal participation to burst patterns suggests that individual neurons were interchangeable in generating the dynamic patterns of bursts, and bursts were coordinated at the population level. We believed that this demonstrates a dynamic routing principle in highly interconnected circuits, in which individual neurons contribute to diverse burst patterns dynamically. Although spikes could be transferred through different neurons, either way the transmission of activity through the same propagation paths would manifest. A major quest for future study is to further elucidate the mechanisms underlying the generation of these ultra-slow oscillations.

## CHAPTER 5

### RECONFIGURATION OF THE BURST COMPOSITION OF ULTRA-SLOW OSCILLATORY ACTIVITY BY LOW-FREQUENCY STIMULATION<sup>§</sup>

We detected repeating burst motifs in the ultra-slow oscillations that spontaneously emerged in our cortical cultures. The analysis was performed by applying a clustering algorithm on the similarity matrices computed based on the latency of individual electrodes during burst initiation. These recurring burst patterns were highly susceptible to external inputs – we observed substantial changes in the burst composition of different motifs upon repetitive stimulation with low-frequency electrical pulses through a pair of substrate embedded electrodes. Changes in these burst patterns over stimulation were significantly greater than those occurring spontaneously in the networks. This finding implies that the emergence of varying motifs of burst propagation in the ultra-slow oscillations could not be accounted by random coincidences of spike trains within the neuronal ensembles. We suggest that perturbation of the ultra-slow oscillations dynamics *in vitro* is an adequate means for the study of *in vivo* mechanisms of plasticity at a population level using electrical and chemical stimulation.

---

<sup>§</sup>Part of this chapter has been submitted as a poster abstract to 42<sup>nd</sup> Annual Meeting of the Society for Neuroscience, New Orleans, LA, 2012.

## 5.1 Introduction

It was earlier proposed that spatiotemporal spike sequences of neuronal ensembles were involved in the coding and the decoding of information (Buzsáki 1989; Abeles 1991). Considerable progress has since been made to understand the nature of temporal coordination of spiking activity among the cell assemblies. There is increasing evidence from the recordings of various brain structures *in vivo* that short conserved spatiotemporal patterns of firing activity were repeatedly expressed and propagated through ensembles of neurons (Prut et al., 1998; Nadasdy et al., 1999; Ikegaya et al., 2004; Luczak et al., 2007). Recurring patterns of activity have also been demonstrated in multiple cortical preparations *in vitro*, which emerged in the form of neuronal avalanches in cortical slices (Beggs and Plenz 2004) as well as ‘motifs’ of bursts in dissociated cultures of cortical neurons (Segev et al., 2004; Madhavan et al., 2007; Rolston et al., 2007; Raichman and Ben-Jacob 2008).

While these repeated dynamics were strongly conserved and could often persist over hours, recent experiments on cortical networks indicate that the recurring burst patterns in cortical networks were considerably altered by external stimuli (Baruchi and Ben-Jacob 2007; Madhavan et al., 2007). Such alterations involved long-lasting changes in the initially stable spatiotemporal patterns of the spontaneous network bursts. This body of work strongly suggests that the recurring patterns of activity in cultured networks could serve as a useful experimental tool for studying plasticity changes in cortical circuits,

and might lead to further insight into the collective dynamics of the networks as a whole.

Here we extended the above work by examining changes induced in the burst patterns of the ultra-slow oscillations in cortical cultures (Mok et al., 2012 [Chapter 4 in this thesis]), with the aim to understand the susceptibility of the oscillatory activity in response to low-frequency electrical stimulation. Our results revealed significantly greater changes in the composition of bursts after sessions of stimulation compared to the spontaneous changes in the networks. This indicates that the application of electrical stimuli affects the intrinsic tendency of the networks in expressing bursts with different propagation patterns, and thus the fundamental properties of the ultra-slow oscillatory activity.

## **5.2 Methods**

### **5.2.1 Cell Culture**

Dense cultures of cortical neurons were prepared on MEAs [see Appendix A for details]. Briefly, cortical tissues were extracted from embryonic (E18) rats and cut into  $1 \text{ mm}^3$  cubes, prior to dissociation into a mixture of neurons and glia using trypsin and trituration. The resulting suspension was diluted to 2500 cells/ $\mu\text{l}$  with tissue culture medium. Subsequently, a 50  $\mu\text{l}$  droplet of the cell suspension was homogeneously spread over the electrode area of each MEA that had been pre-coated with PEI (Sigma). Cultures were sealed with Teflon

lids (Potter and DeMarse 2001) and maintained in Neurobasal-based medium (Invitrogen) inside the incubator.

### **5.2.2 Recording**

We used MEAs (MultiChannel Systems, Reutlingen, Germany) with 60 titanium nitride electrodes, 30  $\mu\text{m}$  in diameter, laid out on a rectangular grid with 200  $\mu\text{m}$  inter-electrode spacing. Signals were amplified using the MEA1060-Inv-BC amplifier (MultiChannel Systems), and sampled at 25 kHz using a commercial data acquisition card (MC\_Card, MultiChannel Systems). The voltage traces were high-pass filtered at 200 Hz, after which spikes were identified by thresholding at 5x estimated standard deviation of the background noise. Duplicate detection of multiphasic spikes was prevented by discarding candidate spikes of smaller amplitude within a  $\pm 1$  ms window. All analysis was performed using our custom Matlab codes.

### **5.2.3 Electrical Stimulation**

Electrical stimuli were generated using our custom-made stimulator [Chapter 3 in this thesis]. Biphasic voltage pulses of  $\pm 800$  mV, 400  $\mu\text{s}$  per phase (positive phase first) were used in this study. Electrical pulses were applied sequentially at 3 seconds interval through two active electrodes in the networks, selected from the electrodes that evoked strong network responses during the pre-experimental screening. The full stimulation sequence lasted 30 minutes. Spontaneous activity was recorded for one hour before and after the

stimulation session. All experiments took place in cultures at 45-55 days *in vitro*. Only cultures that exhibited ultra-slow oscillatory activity throughout the recording periods were used in the subsequent analysis.

#### **5.2.4 Burst Detection**

The algorithm for detecting bursts was adopted from Wagenaar et al. (2005a). Briefly, we searched for the core of bursts by extracting sequences of at least four densely spaced spikes with all ISIs less than 100 ms on individual electrodes. The entourage of spikes on the same electrodes with ISIs less than 200 ms was later included to be part of the bursts. Temporally overlapping burst activity across five or more electrodes was considered a network burst.

#### **5.2.5 Detection of Burst Motifs**

The large variation in the characteristics of bursts in our recordings poses difficulties in identifying independent burst motifs with the standard clustering methods and determining the size of cluster pertaining to each motif. In this study, we represented each motif with a burst cluster of a predefined size that was closest to the averaged representation of the motif, as described in Raichman and Ben-Jacob (2008).

We started by computing the similarity between bursts based on the latencies during which electrodes started to record bursts. The latency between electrode pair  $(i, j)$  during the initiation of burst  $n$ ,  $t_n(i, j)$ , was defined as the

relative difference in the timings of their first spikes in seconds. The similarity index between burst  $n$  and  $m$ ,  $S_{burst}(n, m)$ , was then given by

$$S_{burst}(n, m) = \frac{1}{N_{elc}(N_{elc} - 1)} \sum_{i \neq j} H(t_c - |t_n(i, j) - t_m(i, j)|),$$

where  $H$  is the Heaviside-step function,  $N_{elc}$  is the number of active electrodes, and  $t_c$  is the time threshold.

The similarity indices between bursts were calculated by setting  $t_c = 0.03$  seconds. The sequence of bursts in the resulting similarity matrix was then rearranged using the hierarchical dendrogram method (Press et al., 1992). This produced a new matrix with highly similar bursts located closely in the reordered sequence. All possible clusters each containing  $N_{clus}$  consecutive bursts in the reordered matrix were determined. We set  $N_{clus} = \sqrt{N_{burst}}$  given the total number of bursts,  $N_{burst}$ , in the recordings, since this selection of  $N_{clus}$  was found to be optimum in identifying the presence of well-defined motifs. Each possible cluster was represented by the mean latency of its active electrode pairs across the component bursts, with the mean latency of electrode pair  $(i, j)$ ,  $\bar{t}(i, j)$ , defined as

$$\bar{t}(i, j) = \frac{1}{N_{clus}} \sum_{k \in \kappa} t_k(i, j).$$

The mean similarity within burst cluster  $\kappa$ ,  $S_{clus}(\kappa)$ , was then evaluated by relating

$$S_{clus}(\kappa) = \frac{1}{N_{clus}} \sum_{k \in \kappa} S_{burst}(k, \kappa).$$

The algorithm looked for the burst cluster with the highest value of  $S_{clus}$  as the first motif. To ensure that the selected motif is well defined from other determined clusters, all possible clusters that contained bursts belonging to the previously detected motif or with bursts showing higher similarity with the selected motif than the lowest similarity within the motif itself were removed. The process was repeated iteratively to search for additional motifs with the highest value of  $S_{clus}$  from the remaining clusters.

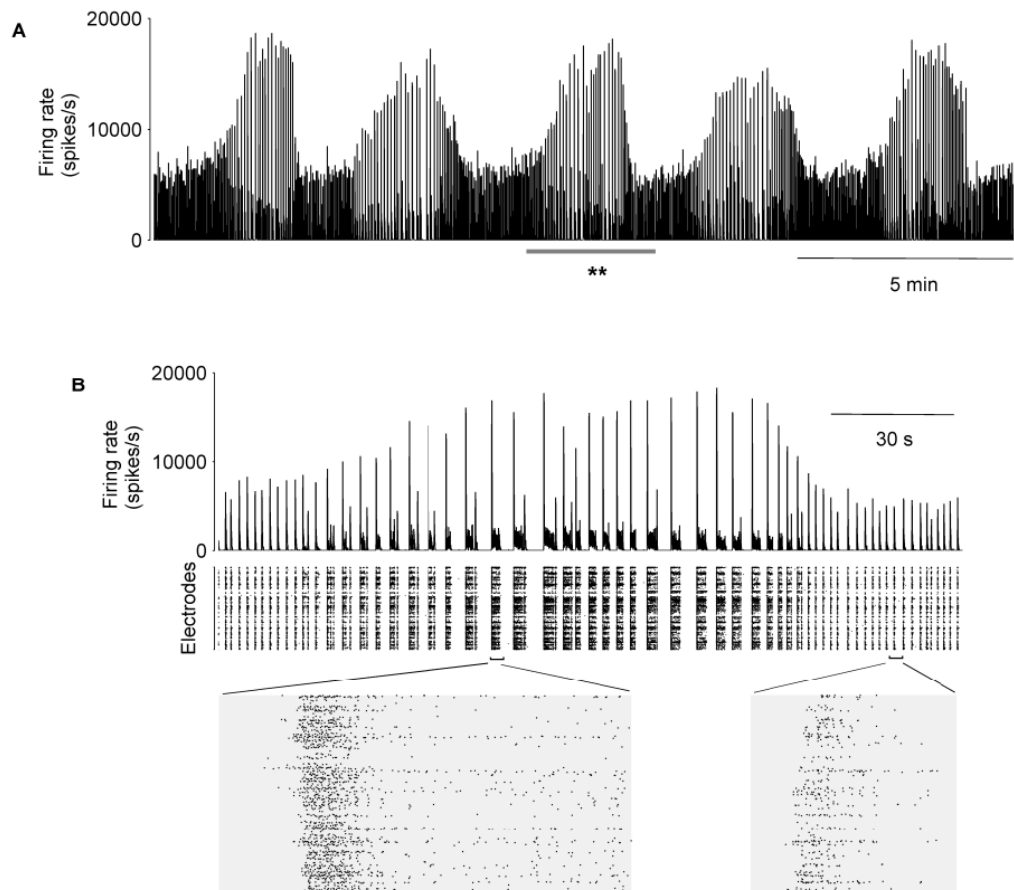
### 5.2.6 Quantifying Changes in Burst Composition

Changes in the composition of bursts across ultra-slow oscillatory activity were determined based on the occurrence of bursts from the identified motifs, using a method adapted from Madhavan et al. (2007). For each motif, we computed the number of its bursting events in 15 minutes sliding windows (with a time step of 30 seconds). This yielded a  $1 \times N$  linear vector, where  $N$  represents the number of time steps for the defined period. A recording with  $M$  identified burst motifs was therefore represented by  $M$  linear vectors, each denoting the occurrence of a single motif. These vectors were then assembled into an  $M \times N$  matrix, constituting an ‘occurrence profile’ for the bursting events.

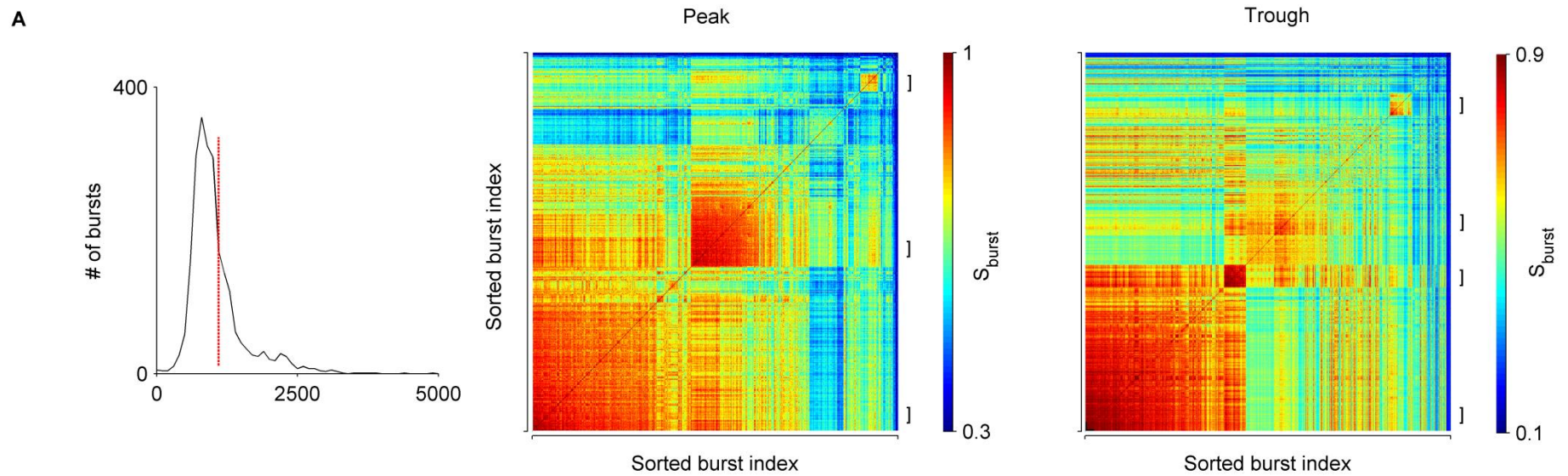
To quantify changes in burst composition that were concomitant with the stimulation sequence, we calculated the mean Euclidean distance of the occurrence profile in the first half period after stimulation to the centroid of the second half period before stimulation. The mean Euclidean distance of the occurrence profile in the second half period before stimulation to the centroid of the first half period before stimulation was also computed, to estimate the magnitude of spontaneous changes in the networks. The significance in the difference between spontaneous changes and changes concomitant with electrical stimulation in the burst composition was then assessed using Wilcoxon signed-rank test.

### **5.3 Results**

Dissociated cortical cultures were found to be spontaneously exhibiting ultra-slow oscillations ( $<0.01$  Hz) in the network-wide aggregate firing rates. Figure 5.1A illustrates how these sequences were organized in alternating up and down states by recurring periods of firing activity. The firing activity was mostly contained in bursts of different sizes that emerged on a timescale of seconds. A closer examination of the temporal structure of these bursts revealed that the latency at which individual electrodes started to record bursts varied slightly from one another, defining a characteristic propagation profile for the bursts (Figure 5.1B). Remarkably, highly stereotyped propagation patterns were repeatedly expressed across the constituent bursts of the ultra-slow oscillatory activity, manifested as multiple burst motifs with distinctive spatiotemporal substructures (Mok et al., 2012 [Chapter 4 in this thesis]).

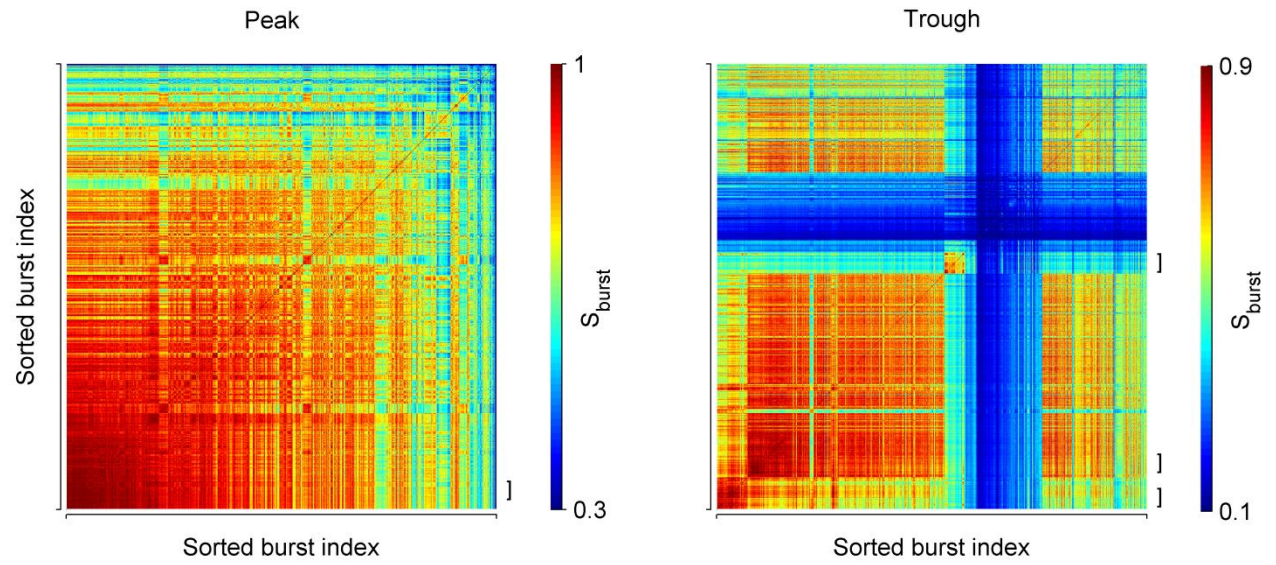
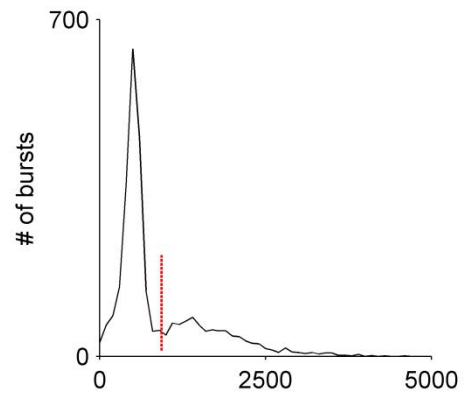


**Figure 5.1:** Ultra-slow oscillations. A. Network-wide aggregate firing rates illustrating the typical ultra-slow oscillations in a 52-day-old culture. The activity of the network was shown to be dominated by population bursts of varying sizes. B. The magnified view of the data segment marked by asterisks in A, and its simultaneous raster plot from 59 electrodes. Insets below show spike raster plots of two individual bursts of different sizes, at 150x magnification of time scale. Note the difference in the latency of the first spikes on individual electrodes from the beginning of each burst.



**Figure 5.2:** (A-C) Identifying repeating burst motifs in the ultra-slow oscillatory activity in three randomly selected cultures. Left: Histogram of number of spikes per burst of all bursts within the two hours period before and after stimulation. Constituent bursts were shown to display a broad range of sizes; they were distinguished as belonging to peaks or troughs according to their sizes by a threshold (denoted by the red line). Figures at the middle and the right are the similarity burst matrices at peaks and troughs, respectively. The order of bursts in these matrices was arranged according to their distance in the correlation space using dendrogram algorithm. Independent burst motifs were identified, marked by “]” at the right of the matrices.

(continued on next page)

**B****(Figure 5.2, continued)**

c

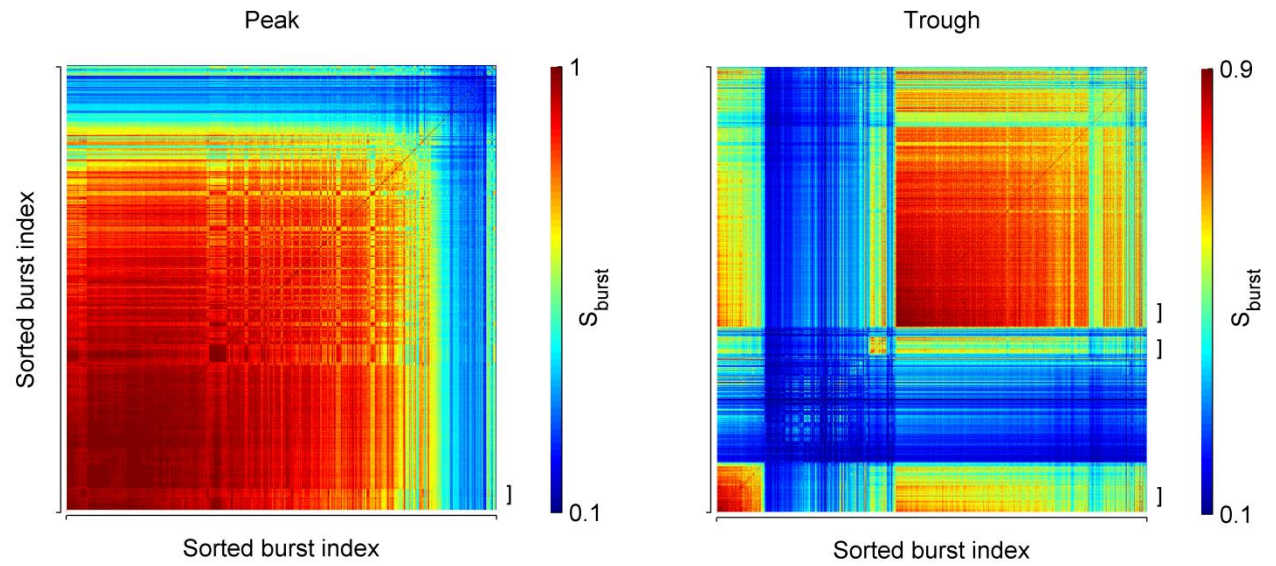
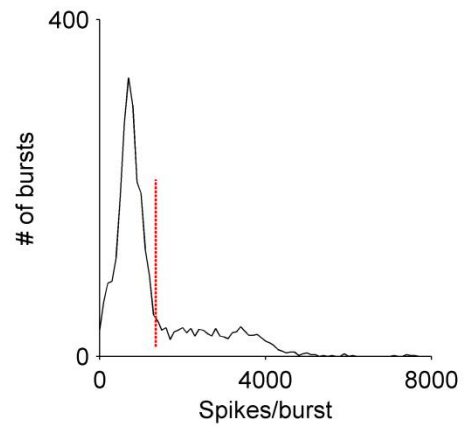


(Figure 5.2, continued)

### 5.3.1 Identifying Recurring Burst Motifs across Stimulation

The propagation profiles of bursts in any given culture were largely diverse, and their characteristics varied considerably from culture to culture. To identify the recurring motifs in the networks across stimulation, the activity propagation patterns of spontaneous bursts during both periods before and after stimulation were compared against each other for similarities, and sorted using a clustering algorithm. Only burst clusters that demonstrated strongly conserved propagation patterns and a good separation with one another were considered as motifs (see Methods). In order to detect motifs of relatively rare events which often remained hidden owing primarily to the wide variety of the burst propagation patterns, the clustering and selection procedures were performed on bursts at peaks and troughs separately. The threshold separating the bursts belonging to peaks and troughs was defined as the average of the number of constituent spikes per burst of all bursts in the recordings. The analysis yielded on average 4-7 motifs in different cultures, characterized by the block-diagonal structures in the reordered similarity matrices (Figure 5.2).

To reaffirm the distinctiveness of the burst motifs at peaks and troughs, we compared the similarities of bursts from all the identified motifs. A higher similarity was observed between bursts within the motifs themselves relative to other motifs (Figure 5.3A), suggesting that the activity propagation patterns of bursts at peaks and troughs were dissimilar. Diversities in the spatiotemporal propagation patterns of bursts from different motifs were

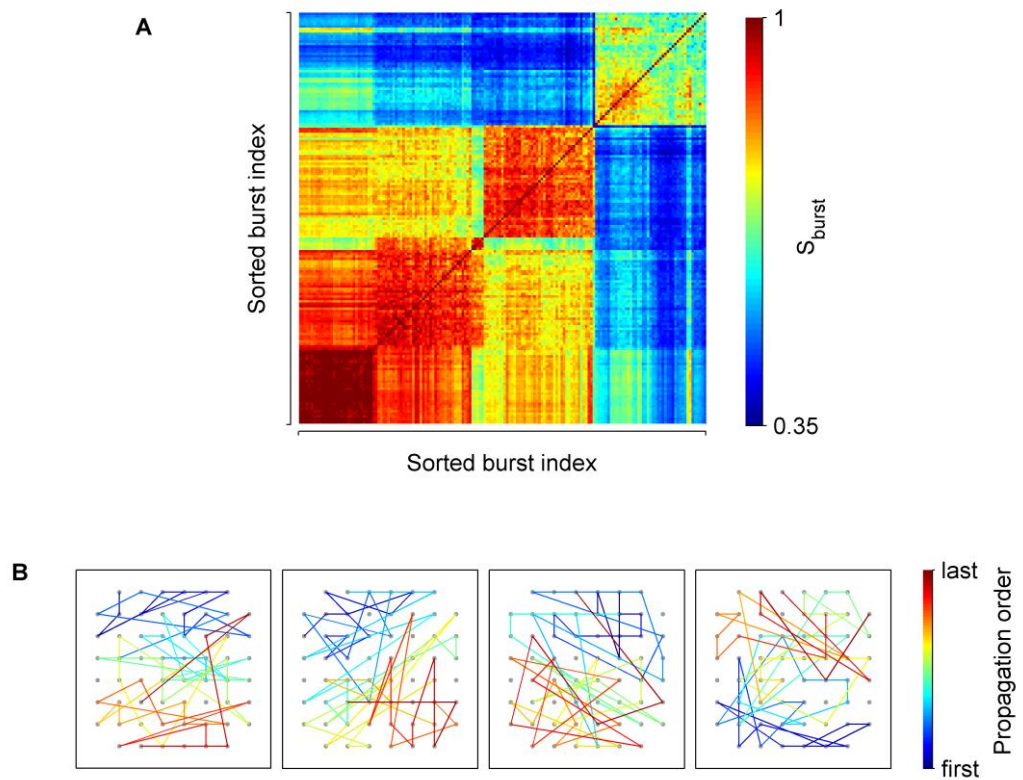


**Figure 5.3:** Distinct propagation patterns of bursts at peaks and troughs. A. Similarity matrix between constituent bursts from all the identified motifs (no rearrangement was made in the order of bursts from their original matrices) in Figure 5.2B. The clear block organization in the matrix suggests that the propagation patterns of individual motifs at peak and trough are dissimilar. B. Activity propagation of bursts (left to right) from the four different motifs in A (left to right). Panels are laid out following the physical geometry of the MEA. Within each panel, the propagation trajectory of the bursting event is displayed, color-coded according to the bar at the right. Notice the distinct propagation pattern in each panel.

indeed evident in Figure 5.3B. Each burst motif was found to associate with a characteristic pattern of propagation trajectory, with the initiation sites of individual motifs distributed over different regions of the networks. This also indicates that there was no single focus from which bursts were initiated in the ultra-slow oscillations.

### **5.3.2 Reconfiguration of the Burst Composition of Ultra-slow Oscillatory Activity**

To determine the distribution of bursts with different propagation patterns, we tracked the time of occurrence of bursts from all the identified motifs. Our results indicate that each of these motifs was composed of bursts from both periods before and after stimulation (Figure 5.4A), indicating that the same burst patterns were continually expressed in the networks after the removal of electrical stimuli. Indeed, strikingly similar propagation patterns could be found in bursts that were separated many minutes apart across stimulation (data not shown). However, it remained to be demonstrated whether the expression of bursts of different propagation patterns was consistent over time, or being altered by electrical stimuli. To visualize the trend of changes, we projected the occurrence profiles of all recording periods on the first two principal vectors obtained from principal component analysis (PCA). Each of these profiles was computed based on the occurrences of bursts from all the identified motifs in the network over its respective time course (see Methods). Inspection of several individual cases revealed that the occurrences of bursts of varying motifs was rather stationary during the periods before and after stimulation compared to the changes across stimulation sessions, as was depicted by the clustering of data in the PCA space (Figure 5.4B).

These intriguing results led us to hypothesize that the application of electrical stimuli might entail significant reconfiguration in the composition of

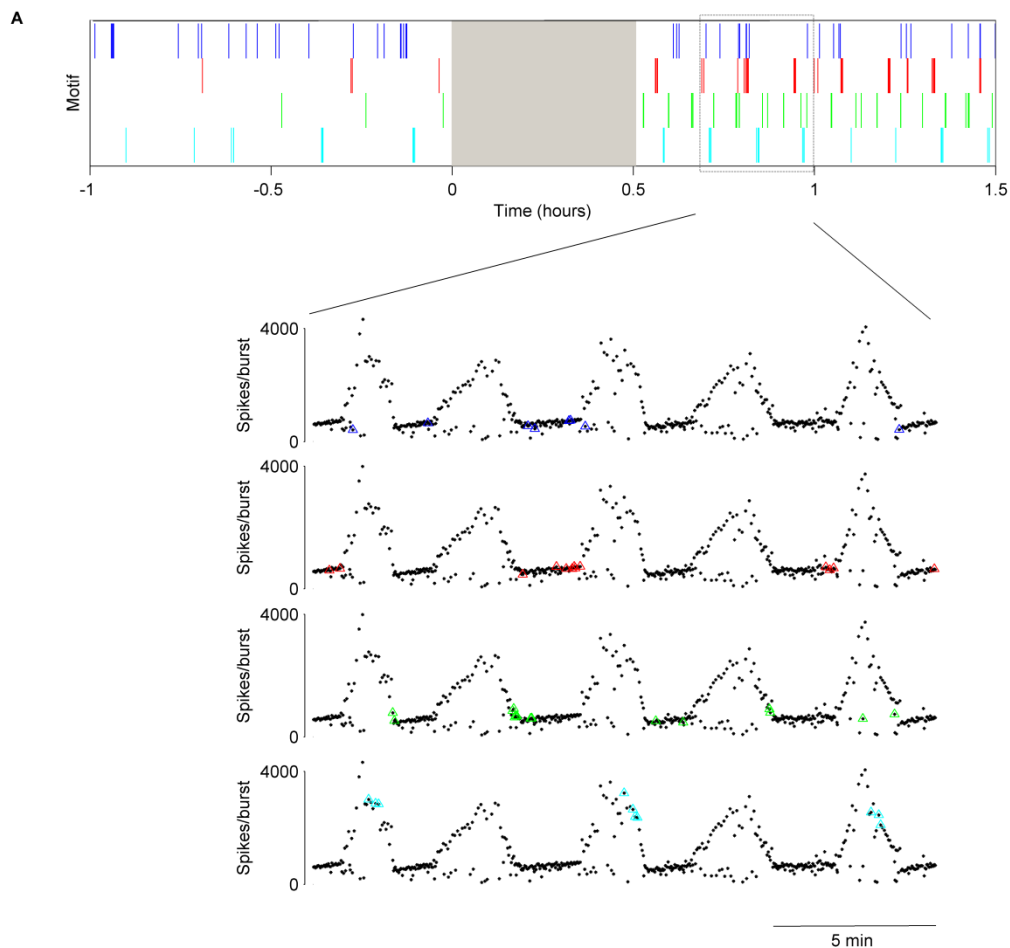


**Figure 5.4:** Distribution of bursts from different motifs across stimulation. A. Raster plot illustrating the temporal locations of bursts from their respective motifs (from the example shown in Figure 5.2B). Each bar marks the occurrence of an individual burst, with the bursting events from each motif assigned a different color. Shaded area indicates the period of stimulation. Inset shows the distribution of bursts from each of the motif across the ultra-slow oscillatory activity at the marked area. Note that bursts from individual motifs were changing in sequential order. B. Projection of occurrence profiles on the first two principal vectors of the PCA algorithm. Each dot represents the occurrence of bursts from an individual time step. The distance between any two dots in the PCA space indicates changes in the burst composition across the corresponding time interval. The time elapsed during the experiment is depicted by the color bar at the bottom.

(continued on next page)

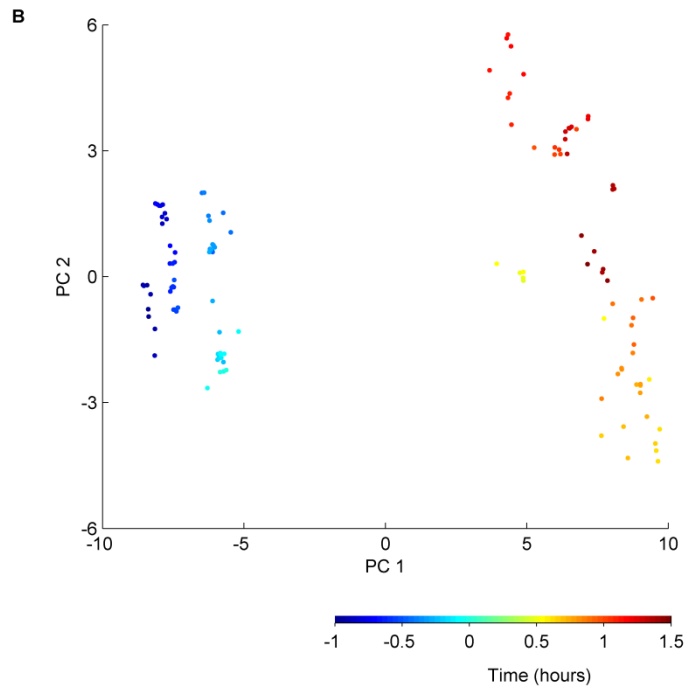


(Figure 5.4, continued)

spontaneous bursts. To quantify the changes, a measure based on the distance of the occurrence profiles in the Euclidean space was used (see Methods). For each experiment, we then calculated the magnitude of spontaneous changes and changes concomitant with the stimulation sequence. Quantification of spontaneous changes is important, as it enables us to estimate the extent of drift or random variability inherent to each culture (Wagenaar et al., 2006c). Changes in the occurrence profiles across stimulation were found to be significantly greater than the changes occurring spontaneously in the networks ( $p < 0.05$ ,  $N = 8$  experiments; Figure 5.5). This indicates that low-frequency stimulation (0.33 Hz) caused alterations in the composition of bursts belonging to different motifs, and hence changes in the collective properties of the ultra-slow oscillatory activity.

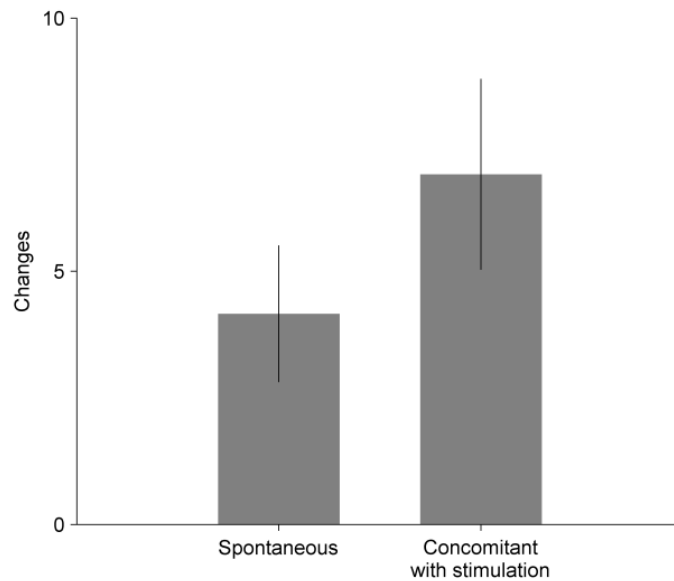


**Figure 5.5:** Comparison of spontaneous changes and changes concomitant with stimulation in the burst composition. Data are mean  $\pm$  sample standard deviation ( $N = 8$  experiments). Wilcoxon signed rank test revealed significant effects of the stimulation sequence ( $p < 0.05$ ).

## 5.4 Discussion

We have earlier shown that the constituent bursts of the ultra-slow oscillatory activity could be clustered into several subgroups of distinct propagation profiles, with bursts from different subgroups manifested in a mixed temporal order of appearance (Mok et al., 2012 [Chapter 4 in this thesis]). However, whether the intrinsic dynamics of these bursting events were resistant to external stimulation is not known. In the present study, we revealed significant changes in the composition of bursts upon repetitive electrical stimulation through a pair of substrate embedded electrodes, thus confirming that the occurrences of bursts with different propagation patterns were highly susceptible to external inputs. This finding also implies that the emergence of varying motifs of burst propagation in the ultra-slow oscillations could not be

accounted by random coincidences of spike trains within the neuronal ensembles.

The widespread existence of repeated dynamics had been revealed in the spontaneous activity of cortical networks *in vivo* and *in vitro* (Abeles 1991; Nadasdy et al., 1999; Segev et al., 2004; Wagenaar et al., 2006a; Luczak et al., 2007; Rolston et al., 2007). However, the mechanisms that generate and maintain such repeating motifs of activity are not yet understood in detail. Several explanations have been proposed on both experimental and theoretical grounds, including existence of intrinsic mechanisms pertaining to cortical circuits (Ikegaya et al., 2004), formation of short-lived functional groups engaging different neurons (Diesmann et al., 1999; Maass et al., 2003; Ikegaya et al., 2004), and spontaneous emergence in self-organizing networks (Rolston et al., 2007). Regardless of the mechanism, the spontaneous formation and persistence of recurring spatiotemporal patterns of activity in the previous preparations and in our cortical cultures strongly suggests that such activity patterns are a robust phenomenon in any large-scale neuronal networks.

It has previously been reported that cortical networks in dissociated cultures demonstrated changes in the recurring burst patterns in response to stimulus presentation (Baruchi and Ben-Jacob 2007; Madhavan et al., 2007). We similarly found changes in the constituent bursts of the ultra-slow oscillations after sessions of electrical stimulation, though the results differed from the above studies with respect to how the activity was modified. We observed a significant reconfiguration in the composition of spontaneous

bursts, while others found evidence of formation and/ or removal of burst motifs. The discrepancy in these findings may reflect a difference in the mode or paradigm of stimulation used, or could be a consequence of how motifs were defined in each study. Changes in these recurring burst patterns have been suggested to reflect alterations in the expression of stored memories (Baruchi and Ben-Jacob 2007; Madhavan et al., 2007), or switches of neural attractor states (Chao et al., 2005; Madhavan et al., 2007; Vajda et al., 2008); however, a full understanding of their physiological roles would require further evidence beyond the data available up till now.

The dynamical changes in the recurring motifs like those observed above present a potential tool for investigating functional plasticity in cortical networks. Moreover, the non-invasive nature of such *in vitro* preparation enables easy manipulation of the network activity with various protocols of electrical stimulation, or with different types of pharmacological agents. Given that recurring burst patterns were also identified in the ultra-slow oscillatory activity, we suggest that perturbation of the ultra-slow oscillations dynamics *in vitro* is an adequate means for the study of *in vivo* mechanisms of plasticity at a population level.

## CHAPTER 6

### CONCLUDING REMARKS AND FUTURE DIRECTION

#### 6.1 Summary of Major Results

##### 6.1.1 Seeding Device

The seeding device offers a new alternative for increasing and controlling the plating density of neuronal cell suspension. I have shown that high-density cortical cultures could be grown on MEAs from cryopreserved neurons of low viability with the aid of this device, and that these cultures demonstrated significant improvements in both their electrophysiological activity and neuronal survival. Ideally, this device should also work on some other cell types or rare cells that come with low concentration.

To review, the major advantages of the seeding device are:

1. Minimal interference: The device is easily detached from MEAs without leaving any residue on the contact surface which might interfere with the cultured networks.
2. Reliable for long-term use: No damage to the fragile electrode tracks on MEAs is found even after repetitive use.

3. Unconstrained process growth: Neuronal processes are allowed to grow freely, unconstrained by any predefined geometry.
4. Simplicity: The device is relatively easy to fabricate, and could be made sterile with any standard protocols.

### **6.1.2 Ultra-slow Oscillations**

Extracellular recordings from cortical cultures revealed a new form of slow rhythm, or “ultra-slow oscillation” that coordinated across a large number of neurons on the timescale of minutes. This finding not only adds to the remarkable range of activity patterns that cortical cultures can exhibit, but provides an additional evidence that neurons could indeed self-organize in dissociated networks. We have focused on the internal structure of firing patterns within the constituent bursts of this slow rhythm, and revealed very interesting dynamics of these rhythmic cultures.

#### *Oscillations Dynamics – Spontaneous and Upon Stimulation*

Using a standard clustering algorithm, we have shown that conserved spatiotemporal patterns of activity were recurrently occurring across the bursts from successive oscillation cycles. Changes in these spatiotemporal dynamics did not occur in discrete time steps, instead different motifs were shown to manifest in a non-uniform order of appearance. Despite the seemingly randomness in their temporal order, consistent motifs of propagation were

shown by the bursts at peaks and troughs. This indicates the existence of fixed propagation paths in which constituent bursts at peaks and troughs were transmitted across the networks, and thus suggests the architecture of the network connectivity as the basis for this emergent oscillatory activity.

By comparing the difference in the motif repetition between multi-unit and single-unit activities, we noted that the consistency of the burst motifs was relatively more robust at the electrode level compared to those at the neuronal level. This is an important finding; it suggests that individual neurons were interchangeable in generating the dynamic patterns of bursts – a demonstration of dynamic routing principle in densely interconnected circuits. Indeed, the same phenomenon has been repeatedly expressed in many *in vitro* and *in vivo* systems. The high reliability shown in these multi-unit activities is very valuable, since they hold the potential to expedite the processing of signals from biological networks, besides being more informative and easily accessible (Supèr and Roelfsema 2005; Stark and Abeles 2007).

To better understand the oscillation dynamics, we studied how their firing activity pattern was modified by electrical stimulation. The stimulation-response experiments revealed that the slow rhythm was readily modified in response to imposed electrical activity, with a significant reconfiguration in the composition of bursts across the ultra-slow oscillations. Since the changes over stimulation were significantly greater than those occurring spontaneously in the networks, we posited that the emergence of varying motifs of burst propagation could not be due to random coincidences of spike trains within the

neuronal ensembles. These experiments provide a direct demonstration of changes in the spatio-temporal activity of the rhythmic cultures, and suggest a potential role of the ultra-slow oscillation dynamics as a means for the study of plasticity mechanisms at the population level.

## **6.2 Future Direction: Towards a Better Understanding of the Ultra-slow Oscillations**

There are many interesting experiments which might aid to enhance our understandings of the ultra-slow oscillations. Several potential ones are listed below.

### **6.2.1 Pharmacology**

Cortical networks growing on MEAs are a good model for studying the effects of various pharmacological agents on the emergent activity patterns. Experiments could be performed to manipulate the ultra-slow oscillations in cortical cultures using drugs that were known to block different modes of synaptic transmission. These studies could possibly shed light on whether and how the intensity and duration of the oscillatory activity is affected by the drug treatments, and help elucidate the role of different receptors in the generation of the slow rhythm.

The effects of a wealth of drugs that might potentially affect the properties of the slow rhythm, such as bicuculline, CNQX, APV, and TTX, to name a few, could be studied.

### **6.2.2 Lithography**

Previous studies on cortical cultures have revealed that the appearance of organizational motifs is strongly dependent on the network architecture (Volman et al., 2005; Raichman and Ben-Jacob 2008). Multiple motifs were exhibited in sufficiently large networks, with a relatively higher number of motifs found in the clustered networks compared to the uniform cultures. Given that ultra-slow oscillations were built on such organizational motifs, it is tantalizing to ask whether the occurrence of the former will similarly be influenced by the imposed network architecture, and if there is a minimum number of neurons required for initializing this activity.

To tackle these questions, one could grow and follow cultures of different sizes on lithographically prepared substrates. Comparing the probability of occurrence of the slow rhythm in these cultures, as well as the developmental periods in which such activity is first initiated, would provide useful hints to the above questions, and yield a fuller picture of how this rhythmic pattern emerge.

## REFERENCES

- Abeles, M., 1991. *Corticonics: Neural circuits of the cerebral cortex*. Cambridge, U. K.: Cambridge University Press.
- Achermann, P. and Borbély, A.A., 1997. Low-frequency (<1 Hz) oscillations in the human sleep electroencephalogram. *Neuroscience*, 81, pp. 213-222.
- Bakkum, D.J., Chao, Z.C. and Potter, S.M., 2008. Spatio-temporal electrical stimuli shape behavior of an embodied cortical network in a goal-directed learning task. *J. Neural Eng.*, 5, pp. 310-323.
- Banker, G. and Goslin, K., 1998. *Culturing nerve cells*, 2<sup>nd</sup> ed. MIT Press, Cambridge, MA.
- Baruchi, I. and Ben-Jacob, E., 2007. Towards neuro-memory-chip: Imprinting multiple memories in cultured neural networks. *Phys. Rev. E*, 75, Art. no.-050901.
- Beggs, J.M. and Plenz, D., 2004. Neuronal avalanches are diverse and precise activity patterns that are stable for many hours in cortical slice cultures. *J. Neurosci.*, 24, pp. 5216-5229.
- Bologna, L.L. et al., 2010. Low-frequency stimulation enhances burst activity in cortical cultures during development. *Neuroscience*, 165, pp. 692-704.
- Buzsáki, G., 1989. Two-stage model of memory trace formation: a role for “noisy” brain states. *Neuroscience*, 31, pp. 551-570.
- Canepari, M. et al., 1997. Experimental analysis of neuronal dynamics in cultured cortical networks and transitions between different patterns of activity. *Biol. Cybern.*, 77, pp. 153-162.
- Chao, Z.C. et al., 2005. Effects of random external background stimulation on network synaptic stability after tetanization: a modeling study. *Neuroinformatics*, 3, pp. 263-280.
- Chao, Z.C., Bakkum, D.J. and Potter, S.M., 2008. Shaping embodied neural networks for adaptive goal-directed behavior. *PLoS Comput. Biol.*, 4, e1000042.
- Claverol-Tinture, E. and Pine, J., 2002. Extracellular potentials in low-density dissociated neuronal cultures. *J. Neurosci. Methods*, 117, pp. 13-21.
- Contreras, D., Timofeev, I. and Steriade, M., 1996. Mechanisms of long-lasting hyperpolarizations underlying slow sleep oscillations in cat corticothalamic networks. *J. Physiol.*, 494, pp. 251-264.

- Corner, M.A. et al., 2002. Physiological effects of sustained blockade of excitatory synaptic transmission on spontaneously active developing neuronal networks – an inquiry into the reciprocal linkage between intrinsic biorhythms and neuroplasticity in early ontogeny. *Neurosci. Biobehav. Rev.*, 26, pp. 127-185.
- Cozzi, L., D'Angelo, P. and Sanguineti, V., 2006. Encoding of time-varying stimuli in populations of cultured neurons. *Biol. Cybern.*, 94, pp. 335-349.
- DeAngelis, G.C., Cumming, B.G. and Newsome, W.T., 1998. Cortical area MT and the perception of stereoscopic depth. *Nature*, 394, pp. 677-680.
- Diesmann, M., Gewaltig, M-O. and Aertsen, A., 1999. Stable propagation of synchronous spiking in cortical neural networks. *Nature*, 402, pp. 529-533.
- Drew, P.J. et al., 2008. Finding coherence in spontaneous oscillations. *Nat. Neurosci.*, 11, pp. 991-993.
- Eytan, D., Brenner, N. and Marom, S., 2003. Selective adaptation in networks of cortical neurons. *J. Neurosci.*, 23, pp. 9349-9356.
- Eytan, D. and Marom, S., 2006. Dynamics and effective topology underlying synchronization in networks of cortical neurons. *J. Neurosci.*, 26, pp. 8465-8476.
- Feinerman, O., Segal, M. and Moses, E., 2007. Identification and dynamics of spontaneous burst initiation zones in unidimensional neuronal cultures. *J. Neurophysiol.*, 97, pp. 2937-2948.
- Furshpan, E.J. and Potter, D.D., 1989. Seizure-like activity and cellular damage in rat hippocampal neurons in cell culture. *Neuron*, 3, pp. 199-207.
- Gibson, S., Judy, J.W. and Marković, D., 2010. Technology-aware algorithm design for neural spike detection, feature extraction and dimensionality reduction. *IEEE Trans. on Neural Syst. and Rehabil. Eng.*, 18, pp. 469-478.
- Gross, G.W., 1979. Simultaneous single unit recording in vitro with a photoetched laser deinsulated gold multimicroelectrode surface. *IEEE Trans. Biomed. Eng.*, 26, pp. 273-279.
- Gross, G., Kowalski, J.M. and Rhoades, B.K., 2000. Spontaneous and evoked oscillations in cultured mammalian neuronal networks. In: Levine, D.S., Brown, V.R., and Shirey, V.T. (eds.). *Oscillations in neural systems*. Lond: L Erlbaum Associates, pp. 3-29.
- Hughes, S.W. et al., 2002. Cellular mechanisms of the slow (<1 Hz) oscillation in thalamocortical neurons in vitro. *Neuron*, 33, pp. 947-958.
- Ikegaya, Y. et al., 2004. Synfire chains and cortical songs: Temporal modules of cortical activity. *Science*, 304, pp. 559-564.

- Jimbo, Y., Tateno, T. and Robinson, H.P.C., 1999. Simultaneous induction of pathway-specific potentiation and depression in networks of cortical neurons. *Biophys. J.*, 76, pp. 670-678.
- Jimbo, Y. et al., 2003. A system for MEA-based multisite stimulation. *IEEE Trans. Biomed. Eng.*, 50, pp. 241-248.
- Jimbo, Y., Kasai, N., Torimitsu, K. and Tateno, T., 2006. MEA-based spike recording in cultured neuronal networks. In: Xing, W.-L., and Cheng, J., (eds.). *Frontiers in biochip technology*. Springer, pp. 88-98.
- Kamioka, H. et al., 1996. Spontaneous periodic synchronized bursting during formation of mature patterns of connections in cortical cultures. *Neurosci. Lett.*, 206, pp. 109-112.
- Kawamoto, J.C. and Barrett, J.N., 1986. Cryopreservation of primary neurons for tissue culture. *Brain Res.*, 384, pp. 84-93.
- Kirov, R. et al., 2009. Slow oscillation electrical brain stimulation during waking promotes EEG theta activity and memory encoding. *Proc. Natl. Acad. Sci. U. S. A.*, 106, pp. 15460-15465.
- Latham, P.E. et al., 2000. Intrinsic dynamics in neuronal networks. II. Experiment. *J. Neurophysiol.*, 83, pp. 828-835.
- Lelong, I.H., Petegnief, V. and Rebel, G., 1992. Neuronal cells mature faster on polyethyleneimine coated plates than on polylysine coated plates. *J. Neurosci. Res.*, 32, pp. 562-568.
- Linke, S. et al., 2006. Aldolase C/zebrin II is released to the extracellular space after stroke and inhibits the network activity of cortical neurons. *Neurochem. Res.*, 31, pp. 1297-1303.
- Lőrincz, M.L. et al., 2009. ATP-dependent infra-slow (<0.1 Hz) oscillations in thalamic networks. *PLoS One*, 4, e4447.
- Luczak, A. et al., 2007. Sequential structure of neocortical spontaneous activity in vivo. *Proc. Natl. Acad. Sci. U. S. A.*, 104, pp. 347-352.
- Maass, W., Natschläger, T. and Markram, H., 2003. Computational models for generic cortical microcircuits. *Neural Comput.*, 14, pp. 2531-2560.
- Madhavan, R., Chao, Z.C. and Potter, S.M., 2007. Plasticity of recurring spatiotemporal activity patterns in cortical networks. *Phys. Biol.*, 4, pp. 181-193.
- Maeda, E., Robinson, H.P.C. and Kawana, A., 1995. The mechanisms of generation and propagation of synchronized bursting in developing networks of cortical neurons. *J. Neurosci.*, 15, pp. 6834-6845.

- Maeda, E. et al., 1998. Modification of parallel activity elicited by propagating bursts in developing networks of rat cortical neurones. *Eur. J. Neurosci.*, 10, pp. 488-496.
- Marom, S. and Shahaf, G., 2002. Development, learning and memory in large random networks of cortical neurons: lessons beyond anatomy. *Q. Rev. Biophys.*, 35, pp. 63-87.
- Marshall, L. et al., 2006. Boosting slow oscillations during sleep potentiates memory. *Nature*, 444, pp. 610-613.
- Metherate, R. and Ashe, J.H., 1993. Ionic flux contributions to neocortical slow waves and nucleus basalis-mediated activation: whole-cell recordings in vivo. *J. Neurosci.*, 13, pp. 5312-5323.
- Misgeld, U., Zeilhofer, H.U. and Swandulla, D., 1998. Synaptic modulation of oscillatory activity of hypothalamic neuronal networks in vitro. *Cell Mol. Neurobiol.*, 18, pp. 29-43.
- Mok, S.Y. et al., 2012. Ultra-slow oscillations in cortical networks in vitro. *Neuroscience*, 206, pp. 17-24.
- Mtetwa, N. and Smith, L.S., 2006. Smoothing and thresholding in neuronal spike detection. *Neurocomputing*, 69, pp. 1366-1370.
- Murphy, T.H. et al., 1992. Spontaneous synchronous synaptic calcium transients in cultured cortical neurons. *J. Neurosci.*, 12, pp. 4834-4845.
- Nádasdy, Z. et al., 1999. Replay and time compression of recurring spike sequences in the hippocampus. *J. Neurosci.*, 19, pp. 9497-9507.
- Nadasdy, Z. et al., 2002. Comparison of unsupervised algorithms for on-line and off-line spike sorting, in *32<sup>nd</sup> Annual Meeting of the Society for Neuroscience*, Orlando, FL.
- Novak, J.L. and Wheeler, B.C., 1988. Multisite hippocampal slice recording and stimulation using a 32 element microelectrode array. *J. Neurosci. Methods*, 23, pp. 149-159.
- Opitz, T., De Lima, A.D. and Voigt, T., 2002. Spontaneous development of synchronous oscillatory activity during maturation of cortical networks in vitro. *J. Neurophysiol.*, 88, pp. 2196-2206.
- Otto, F. et al., 2003. Cryopreserved rat cortical cells develop functional neuronal networks on microelectrode arrays. *J. Neurosci. Methods*, 128, pp. 173-181.
- Pasquale, V. et al., 2008. Self-organization and neuronal avalanches in networks of dissociated cortical neurons. *Neuroscience*, 153, pp. 1354-1369.

- Patel, D., Ford, T.C. and Rickwood, D., 1998. Fractionation of cells by sedimentation methods. In: Fisher, D., Francis, G.E., and Rickwood, D. (eds.). *Cell separation: a practical approach*. Oxford University Press, pp. 43-89.
- Penttonen, M. et al., 1999. Ultra-slow oscillation (0.025 Hz) triggers hippocampal afterdischarges in Wistar rats. *Neuroscience*, 94, pp. 735-743.
- Pine, J., 1980. Recording action potentials from cultured neurons with extracellular microcircuit electrodes. *J. Neurosci. Methods*, 2, pp. 19-31.
- Potter, S.M., 2001. Distributed processing in cultured neuronal networks. In: Nicolelis, M.A.L. (ed.). *Progress in Brain Research*. Vol. 130. Elsevier Science, pp. 49-62.
- Potter, S.M. and DeMarse, T.B., 2001. A new approach to neural cell culture for long-term studies. *J. Neurosci. Methods*, 110, pp. 17-24.
- Press, W.H., Teukolsky, S.A., Vetterling, W.T. and Flannery, B.P., 1992. Numerical recipes in C. Cambridge: Cambridge University Press.
- Prut, Y. et al., 1998. Spatiotemporal structure of cortical activity: Properties and behavioral relevance. *J. Neurophysiol.*, 79, pp. 2857-2874.
- Quiroga, R.Q., Nadasdy, Z. and Ben-Shaul, Y., 2004. Unsupervised spike detection and sorting with wavelets and superparamagnetic clustering. *Neural Comput.*, 16, pp. 1661-1687.
- Raichman, N. and Ben-Jacob, E., 2008. Identifying repeating motifs in the activation of synchronized bursts in cultured neuronal networks. *J. Neurosci. Methods*, 170, pp. 96-110.
- Ramakers, G.J.A. et al., 1991. Development of neurons and glial cells in cerebral cortex, cultured in the presence or absence of bioelectric activity: morphological observations. *Eur. J. Neurosci.*, 3, pp. 140-153.
- Regehr, W.G. et al., 1989. Sealing cultured invertebrate neurons to embedded dish electrodes facilitates long-term stimulation and recording. *J. Neurosci. Methods*, 30, pp. 91-106.
- Reig, R. et al., 2010. Temperature modulation of slow and fast cortical rhythms. *J. Neurophysiol.*, 103, pp. 1253-1261.
- Robinson, H.P. et al., 1993. Periodic synchronized bursting and intracellular calcium transients elicited by low magnesium in cultured cortical neurons. *J. Neurophysiol.*, 70, pp. 1606-1616.
- Rolston, J.D., Wagenaar, D.A. and Potter, S.M., 2007. Precisely timed spatiotemporal patterns of neural activity in dissociated cortical cultures. *Neuroscience*, 148, pp. 294-303.

- Rolston, J.D., Gross, R.E. and Potter, S.M., 2009. A low-cost multielectrode system for data acquisition enabling real-time closed-loop processing with rapid recovery from stimulation artifacts. *Frontiers in Neuroengineering*, 2, pp. 1-17.
- Sanchez-Vives, M.V. and McCormick, D.A., 2000. Cellular and network mechanisms of rhythmic recurrent activity in neocortex. *Nat. Neurosci.*, 3, pp. 1027-1034.
- Segal, M.M., Baugman, R.W., Jones, K.A. and Huettner, J.E., 1998. Mass cultures and microislands of neurons from postnatal rat brain. In: Banker, G., and Goslin, K. (eds.). *Culturing nerve cells*. MIT Press, Cambridge, pp. 309-338.
- Segev, R. et al., 2004. Hidden neuronal correlations in cultured networks. *Phys. Rev. Lett.*, 92, Art. no.- 118102.
- Shahaf, G. and Marom, S., 2001. Learning in networks of cortical neurons. *J. Neurosci.*, 21, pp. 8782-8788.
- Shefi, O. et al., 2002. Morphological characterization of in vitro neuronal networks. *Phys. Rev. E*, 66, Art. no.-021905.
- Shu, Y., Hasenstaub, A. and McCormick, D.A., 2003. Turning on and off recurrent balanced cortical activity. *Nature*, 423, pp. 288-293.
- Stark, E. and Abeles, M., 2007. Predicting movement from multiunit activity. *J. Neurosci.*, 27, pp. 8387-8394.
- Steriade, M. et al., 1993a. The slow (<1 Hz) oscillation in reticular thalamic and thalamocortical neurons: scenario of sleep rhythm generation in interacting thalamic and neocortical networks. *J. Neurosci.*, 13, pp. 3284-3299.
- Steriade, M., Nuñez, A. and Amzica, F., 1993b. A novel slow (<1 Hz) oscillation of neocortical neurons in vivo: depolarizing and hyperpolarizing components. *J. Neurosci.*, 13, pp. 3252-3265.
- Streit, J. et al., 2001. The generation of rhythmic activity in dissociated cultures of rat spinal cord. *Eur. J. Neurosci.*, 14, pp. 191-202.
- Supèr, H. and Roelfsema, P., 2005. Chronic multiunit recordings in behaving animals: advantages and limitations. *Progress in Brain Research*, 147, pp. 263-281.
- Tam, D.C., 2000. Detection of oscillations and synchronous firing in neurons. In: Levine, D.S., Brown, V.R., and Shirey, V.T. (eds.). *Oscillations in neural systems*. Lawrence Erlbaum Associates, pp. 31-49.

- Thomas, Jr.C.A. et al., 1972. A miniature microelectrode array to monitor the bioelectric activity of cultured cells. *Exp. Cell Res.*, 74, pp. 61-66.
- Timofeev, I. et al., 2000. Origin of slow cortical oscillations in deafferented cortical slabs. *Cereb. Cortex*, 10, pp. 1185-1199.
- Vajda, I. et al., 2008. Low-frequency stimulation induces stable transitions in stereotypical activity in cortical networks. *Biophys. J.*, 94, pp. 5028-5039.
- van Ooyen, A., van Pelt, J. and Corner, M.A., 1995. Implications of activity-dependent neurite outgrowth for neuronal morphology and network development. *J. Theor. Biol.*, 172, pp. 63-82.
- van Pelt, J. et al., 2005. Dynamics and plasticity in developing neuronal networks in vitro. *Brain Res.*, 147, pp. 173-188.
- Vanhatalo, S. et al., 2004. Infralow oscillations modulate excitability and interictal epileptic activity in the human cortex during sleep. *Proc. Natl. Acad. Sci. U. S. A.*, 101, pp. 5053-5057.
- Voigt, T., Baier, H. and de Lima, A.D., 1997. Synchronization of neuronal activity promotes survival of individual rat neocortical neurons in early development. *Eur. J. Neurosci.*, 9, pp. 990-999.
- Volman, V., Baruchi, I. and Ben-Jacob, E., 2005. Manifestation of function-follow-form in cultured neuronal networks. *Phys. Biol.*, 2, pp. 98-110.
- Wagenaar, D.A. and Potter, S.M., 2002. Real-time multi-channel stimulus artifact suppression by local curve fitting. *J. Neurosci. Methods*, 120, pp. 113-120.
- Wagenaar, D.A. and Potter, S.M., 2004. A versatile all-channel stimulator for electrode arrays, with real-time control. *J. Neural Eng.*, 1, pp. 39-44.
- Wagenaar, D.A., DeMarse, T.B. and Potter, S.M., 2005a. MEABench: A toolset for multi-electrode data acquisition and on-line analysis, in *Proc. 2<sup>nd</sup> Intl. IEEE EMBS Conf. on Neural Eng.*, pp. 518-521.
- Wagenaar, D.A. et al., 2005b. Controlling bursting in cortical cultures with closed-loop multi-electrode stimulation. *J. Neurosci.*, 25, pp. 680-688.
- Wagenaar, D.A., 2006. *Development and control of epileptiform bursting in dissociated cortical cultures*, Ph. D. Thesis, California Institute of Technology.
- Wagenaar, D.A., Nadasdy, Z. and Potter, S.M., 2006a. Persistent dynamic attractors in activity patterns of cultured neuronal networks. *Phys. Rev. E Stat. Nonlin. Soft Matter Phys.*, 73, Art. no.-051907.

- Wagenaar, D.A., Pine, J. and Potter, S.M., 2006b. An extremely rich repertoire of bursting patterns during the development of cortical cultures. *BMC Neurosci.*, 7, Art. no.- 11.
- Wagenaar, D.A., Pine, J. and Potter, S.M., 2006c. Searching for plasticity in dissociated cortical cultures on multi-electrode arrays. *J. Neg. Results Biomed.*, 5, 16.
- Weliky, M. and Katz, L.C., 1999. Correlational structure of spontaneous neuronal activity in the developing lateral geniculate nucleus in vivo. *Science*, 285, pp. 599-604.
- Wyart, C., Ybert, C., Douarche, C., Herr, C., Chatenay, D. and Bourdieu, L., 2005. A new technique to control the architecture of neuronal networks in vitro. In: Poindron, P., Piguet, P., and Förster, E. (eds.). *New methods for culturing cells from nervous tissues*. Basel: Karger, pp. 23-57.
- Zhu, G. et al., 2010. Transient alterations in slow oscillations of hippocampal networks by low-frequency stimulations on multi-electrode arrays. *Biomed. Microdevices*, 12, pp. 153-158.

## APPENDIX A

### CULTURING METHODS

#### **Tissue Extraction**

A timed-pregnant Wistar rat (E18) was euthanized using CO<sub>2</sub>. A quick C-section was performed and the uterus was placed in an ice embedded petri dish. Brains were removed from the embryos and stored in slushy (near frozen) oxygenated Hanks' balanced salt solution (Invitrogen, 14170-112). The entire neocortex, excluding the hippocampus was then dissected under sterile condition. Cortices were stored at 4 °C in Hibernate E (BrainBits).

#### **Cell Dissociation**

Cortices were cut into ~1 mm<sup>3</sup> pieces and transferred, in a small volume, by a wide-bore pipette tip into recently thawed 0.25% trypsin (Invitrogen, 15050-065). The trypsin was allowed to work at 37 °C for 15 minutes. The cortical chunks were then transferred as before to 1 ml Hanks' balanced salt solution that was added with 10% Equine serum (HyClone, SH30074.03). They were triturated by passing through a 1 ml pipette tip 6-10 times in sets of 2 or 3. The pieces were allowed to settle in between sets and the suspended cells were transferred to a new 15 ml tube. The cell suspension was then spun down onto bovine serum albumin (Sigma, B3156; 1% in PBS) at 150xg for 6 minutes.

The supernatant was discarded, and the cells were resuspended in culturing medium. The suspension was then slowly passed through a 40  $\mu\text{M}$  cell strainer (Falcon, 35-2340) to remove the left-over clumps. They were diluted to 2500 cells/ $\mu\text{l}$  with culturing medium.

### **Preparation of MEA Surface**

1. Cleaning: Clean with 2% Tergazyme solution (Alconox) for 15 minutes, and rinse thoroughly with ddH<sub>2</sub>O.
2. Sterilization: Autoclave at 121  $^{\circ}\text{C}$  for 10 minutes.
3. Coating:

750 ml PEI solution (recipe below) was applied to each of the MEA. All the dishes were covered and incubated overnight at 37  $^{\circ}\text{C}$ . On the next day, PEI was removed and the MEAs were rinsed thoroughly with ddH<sub>2</sub>O for three times, filling and aspirating the dishes with 1-2 ml each time. They were then let completely dry on the laminar hood. The dishes were sterilized by 5 minutes of UV before use.

### ***Recipe for PEI Solution***

PEI solution: 0.05% (by weight) poly-ethylene-imine (from 50% w/v aqueous solution) in borate buffer solution (BBS).

BBS: 3.1 g boric acid plus 4.75 g borax in 1 liter ddH<sub>2</sub>O. Adjust pH to 8.4. Filter sterilize at 0.2  $\mu\text{m}$ .

#### Reagents description:

1. Poly-ethylene-imine: Sigma, P-3143
2. Borax (sodium tetraborate): Sigma, B-0127 (anhydrous 99%)
3. Boric acid: Fisher Scientific, A73-500

#### **Plating**

The cell suspension was added with 20  $\mu$ l of 1 mg/ml laminin, and thoroughly mixed with a vortex mixer for about 20 seconds. Subsequently, a drop of 50  $\mu$ l cell suspension was added onto the central area of each MEA that has been treated with PEI. All the dishes were immediately sealed with FEP<sup>®</sup> Teflon membranes and transferred to an incubator (37  $^{\circ}$ C, 5% CO<sub>2</sub>). Cultures were left for 2 hours to allow cell attachment. 1 ml of culturing medium was then added to each dish.

#### ***Recipe for Neurobasal Culturing Medium***

Mix the following in a 50 ml centrifuge tube:

Reagent	Quantity (ml)	Vendor
Neurobasal Medium	45	Invitrogen, 21103-049
B27	1	Invitrogen, 17504-044
Glutamax	0.13	Invitrogen, 35050-061
Equine Serum	2.5	HyClone, SH30074.03

## Maintenance

On DIV7, 0.5 ml old medium was removed from each culture and replaced with the same amount of fresh Neurobasal medium. Subsequent medium replacement was carried out every 4-6 days, depending on the changes in the color of the medium. No antimetabolic drug was added to restrict glia cell proliferation, as they were known to be important for maintaining long-term culture health. To prevent infection, the Teflon cover was replaced with a freshly autoclaved one every time after feeding.

## Recording

All recordings were performed inside the same incubator in which the cultures were maintained. The pre-amplifier was placed on top of a custom-made heat exchanger (Figure A.1) that was water-cooled with running water from a tap to dissipate the excess heat.

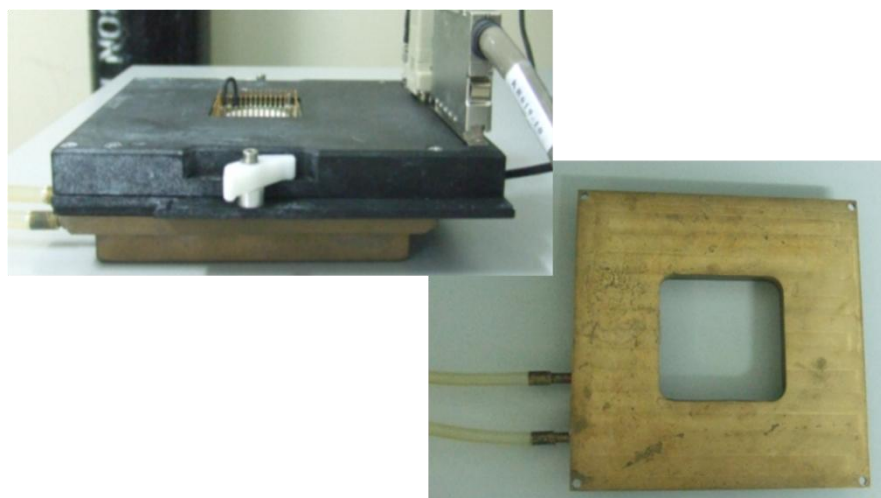


**Figure A.1:** Photograph showing the amplifier placed on top of the custom-made heat exchanger.